Energetically Demanding Transport in a Supramolecular Assembly

Chuyang Cheng,[†] Paul R. McGonigal,[†] Wei-Guang Liu,[‡] Hao Li,[†] Nicolaas A. Vermeulen,[†] Chenfeng Ke,[†] Marco Frasconi,[†] Charlotte L. Stern, [†] William A. Goddard III,[‡] J. Fraser Stoddart[†*]

[†] Department of Chemistry, Northwestern University, 2145 Sheridan Road, Evanston, Illinois 60208, United States
[‡] Materials and Process Simulation Center, California Institute of Technology, Pasadena, California 91125, United States

* Email: stoddart@northwestern.edu

SUPPORTING INFORMATION

Table of Contents

1. General Methods S2
2. Synthetic Procedures S2
3. UV/Vis/NIR Spectroscopy S19
4. Single Crystal X-Ray Diffraction S20
5. 1H NMR Spectroscopy Investigation of Pumping and Dethreading S21
6. DFT Calculations S31
7. Calculation of Energy Conversion Efficiency S49
8. References S51

1. General Methods

All reagents were purchased from commercial suppliers (Sigma-Aldrich or Fisher) and employed without further purification. Cyclobis(paraquat-*p*-phenylene) tetrakis(hexafluorophosphate)[1] (**CBPQT**•4PF_6), **S6**[2] and **S8**•2PF_6[3] were prepared according to literature procedures. Thin layer chromatography (TLC) was performed on silica gel 60 F254 (E. Merck). Column chromatography was carried out on silica gel 60F (Merck 9385, 0.040–0.063 mm). Solvents used in experiments involving radicals were degassed using the freeze-pump-thaw method. UV/Vis/NIR Spectra were recorded on a Varian 100-Bio UV-Vis spectrophotometer in MeCN at room temperature. Nuclear magnetic resonance (NMR) spectra were recorded on Bruker Avance 600 or Varian P-Inova 500 spectrometers, with working frequencies of 600 and 500 MHz for ^{1}H, and 150 and 125 MHz for ^{13}C nuclei, respectively. Chemical shifts are reported in ppm relative to the signals corresponding to the residual non-deuterated solvents ($CDCl_3$: δ = 7.26 ppm, CD_3CN: δ =1.94 ppm). High resolution mass spectra were measured on a Finnigan LCQ iontrap mass spectrometer (HR-ESI).

2. Synthetic Procedures

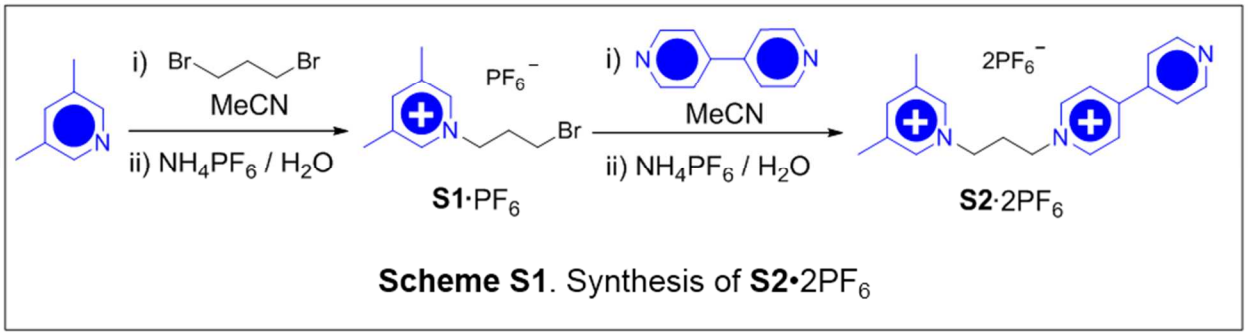

Scheme S1. Synthesis of **S2**•2PF_6

S1•PF_6: A mixture of 3,5-lutidine (1.07 g, 10 mmol) and 1,3-dibromopropane (20 mL) was stirred at 120 °C overnight. After cooling to room temperature, the mixture was poured into Et_2O (50 mL). The resulting suspension was extracted with H_2O (3 × 20 mL), then NH_4PF_6 (2 g) was added to the combined aqueous phase. The precipitate was filtered and washed with H_2O (3 x 5 mL) to afford **S1**•PF_6 (3.28 g, 88%). ^{1}H NMR (500 MHz, CD_3CN): δ 8.36 (s, 2H), 8.15 (s, 1H),

4.54 (t, J = 7.2 Hz, 2H), 3.47 (t, J = 6.4 Hz, 2H), 2.52 – 2.47 (m 8H). ^{13}C NMR (126 MHz, CD_3CN): δ 147.5, 142.1, 139.8, 60.3, 33.6, 29.4, 17.9. ESI-HRMS calcd for m/z = 228.03879 [M – PF_6]$^+$, found m/z = 228.03932.

S2•2PF_6: A mixture of **S1**•PF_6 (1.87 g, 5 mmol) and 4,4′-bipyridine (0.78 g, 5 mmol) were stirred in MeCN (15 mL) for 2 days. After cooling to room temperature, the mixture was poured into Et_2O (50 mL). The resulting suspension was filtered and washed with Et_2O (3 × 5 mL). The solid was dissolved in H_2O (50 mL), then NH_4PF_6 (2 g) was added. The precipitate was filtered and washed with H_2O (3 × 5 mL) to afford a crude product, which was purified by column chromatography (SiO_2 : MeOH / NH_4Cl (aq, 2M) / $MeNO_2$ = 7:2:1), followed by counterion exchange (NH_4PF_6 / H_2O) to afford **S2**•2PF_6 (1.35 g, 45%) as a white solid. ^{1}H NMR (500 MHz, CD_3CN): δ 8.86 (d, J = 6.2 Hz, 2H), 8.77 (d, J = 6.7 Hz, 2H), 8.40 – 8.33 (m, 4H), 8.19 (s, 1H), 7.80 (d, J = 6.3 Hz, 2H), 4.64 (t, J = 7.6 Hz, 2H), 4.54 (t, J = 7.6 Hz, 2H), 2.64 (p, J = 7.2 Hz, 2H), 2.49 (s, 6H). ^{13}C NMR (126 MHz, CD_3CN): δ 155.3, 151.8, 147.8, 145.6, 142.0, 141.6, 140.0, 126.9, 122.4, 58.3 (2×C), 32.2, 18.0. ESI-HRMS calcd for m/z = 450.15338 [M – PF_6]$^+$, found m/z = 450.15382.

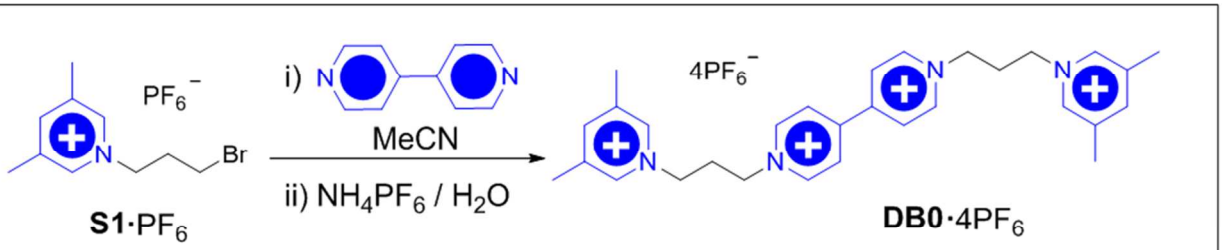

Scheme S2. Synthesis of **DB0**•2PF_6

DB0•4PF_6: A mixture of **S1**•PF_6 (185 mg, 0.5 mmol) and 4,4′-bipyridine (30 mg, 0.19 mmol) were stirred in MeCN (1 mL) for 7 days. After cooling to room temperature, the mixture was poured into Et_2O (50 mL). The resulting suspension was filtered and washed with Et_2O (3 × 5

mL). The solid was dissolved in H_2O (50 mL), and then NH_4PF_6 (2 g) was added. The precipitate was filtered and washed with H_2O (3 × 5 mL) to afford a crude product, which was purified by column chromatography (SiO_2 : MeOH / NH_4Cl (aq, 2M) / $MeNO_2$ = 7:2:1), followed by counterion exchange (NH_4PF_6 / H_2O) to afford **S3**•4PF_6 (1.35 g, 45%) as a colorless solid. ^{1}H NMR (500 MHz, CD_3CN): δ 8.91 (d, J = 6.9 Hz, 4H), 8.44 (d, J = 6.9 Hz, 4H), 8.38 (s, 4H), 8.20 (s, 2H), 4.70 (t, J = 8.0 Hz, 4H), 4.55 (d, J = 7.9 Hz, 4H), 2.71 – 2.59 (m, 4H), 2.50 (s, 12H). ^{13}C NMR (126 MHz, CD_3CN): δ 150.0, 146.9, 145.5, 141.1, 139.1, 127.2, 58.0, 57.3, 31.3, 17.1. ESI-HRMS calcd for m/z = 889.20213 $[M - PF_6]^+$, found m/z = 889.20283.

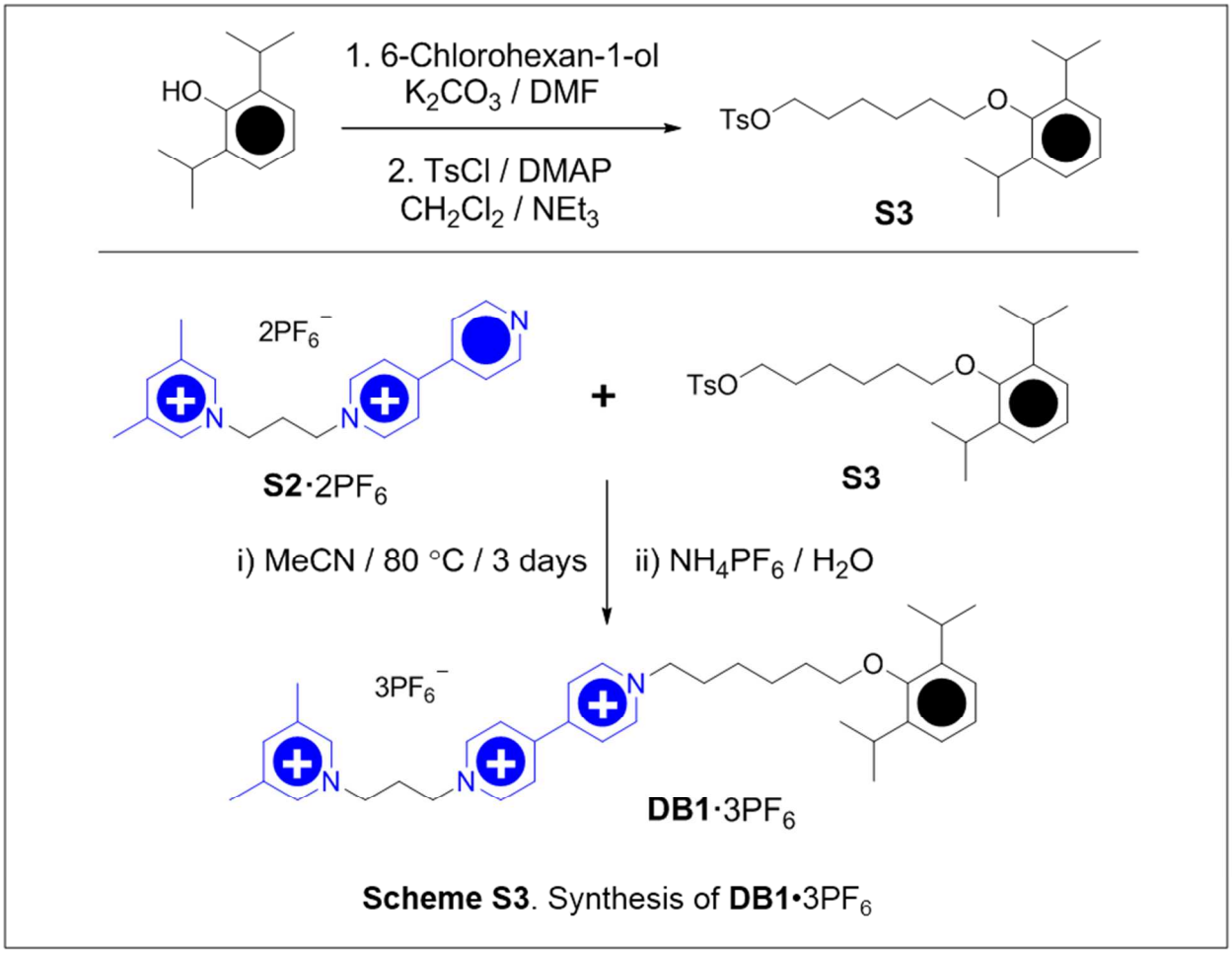

Scheme S3. Synthesis of **DB1**•3PF_6

S3: A mixture of 2,6-diisopropylphenol (1.78 g, 10 mmol), 6-chlorohexan-1-ol (1.36 g, 10 mmol) and K_2CO_3 (3.0 g, 22 mmol) was stirred at 100 °C in DMF (30 mL) overnight. After cooling to room temperature, the mixture was poured into H_2O (100 mL). The resulting mixture was extracted with CH_2Cl_2 (3 × 30 mL) and the combined organic phases were washed with saturated aqueous NaCl solution (100 mL). After drying ($MgSO_4$), the solvent was removed in vacuo to afford a crude precursor (2.6 g) as a light-yellow oil. The crude precursor alcohol, *p*-toluenesulfonyl chloride (2.0 g, 10.5 mmol) and 4-dimethylaminopyridine (122 mg, 1 mmol) were stirred in Et_3N (5 mL) and CH_2Cl_2 (50 mL) at room temperature for 3 h. The solution was poured into H_2O (50 mL). The resulting mixture was extracted with CH_2Cl_2 (3 × 30 mL) and the combined organic phases were washed with saturated aqueous NaCl solution (50 mL). After drying ($MgSO_4$), the solvent was removed in vacuo and the resulting residue was purified by column chromatography (SiO_2: Hexanes / EtOAc 5:1) to afford **S3** (3.0 g, 69%). ^{1}H NMR (500 MHz, $CDCl_3$) δ 7.80 (d, J = 8.0 Hz, 2H), 7.34 (d, J = 7.9 Hz, 2H), 7.17 – 6.99 (m, 3H), 4.06 (t, J = 6.4 Hz, 2H), 3.69 (t, J = 6.4 Hz, 2H), 3.27 (hept, J = 6.9 Hz, 2H), 2.44 (s, 3H), 1.82 – 1.74 (m, 2H), 1.71 (p, J = 6.7 Hz, 2H), 1.52 – 1.45 (m, 2H), 1.42 (m, 2H), 1.21 (d, J = 6.9 Hz, 12H). ^{13}C NMR (126 MHz, $CDCl_3$) δ 153.3, 144.7, 141.8, 133.2, 129.8, 127.9, 124.4, 123.9, 74.5, 70.5, 30.2, 28.9, 26.4, 25.6, 25.4, 24.1, 21.7. ESI-HRMS calcd for m/z = 432.23343 $[M + H]^+$, found m/z = 432.23356.

DB1•3PF_6: A mixture of **S2**•2PF_6 (100 mg, 0.17 mmol) and **S3** (100 mg, 0.23 mmol) was stirred at 80 °C in MeCN (1 mL) for 3 days. After cooling to room temperature, the solvent was removed under reduced pressure. The resulting residue was purified by column chromatography (SiO_2 : MeOH / NH_4Cl (aq, 2M) / $MeNO_2$ = 7:2:1), followed by counterion exchange (NH_4PF_6 / H_2O) to afford **DB1**•3PF_6 (100 mg, 60%). ^{1}H NMR (500 MHz, CD_3CN): δ 8.94 – 8.89 (m, 4H), 8.42 (d, J = 6.9 Hz, 2H), 8.40 – 8.36 (m, 4H), 8.21 (s, 1H), 7.14 – 7.05 (m, 3H), 4.69 (t, J = 8.0

Hz, 2H), 4.65 (t, J = 7.5 Hz, 2H), 4.55 (t, J = 7.5 Hz, 2H), 3.73 (t, J = 6.4 Hz, 2H), 3.30 (hept, J = 6.9 Hz, 2H), 2.65 (p, J = 7.2 Hz, 2H), 2.50 (s, 6H), 2.11 – 2.03 (m, 2H), 1.87 – 1.76 (m, 2H), 1.61 (m, 2H), 1.53 – 1.44 (m, 2H), 1.19 (d, J = 6.9 Hz, 12H). ^{13}C NMR (126 MHz, CD_3CN): δ 153.9, 151.1, 150.3, 147.8, 146.4, 146.2, 142.4, 142.0, 140.1, 128.1, 127.8, 125.1, 124.6, 75.0, 62.7, 58.9, 58.2, 32.2, 31.5, 30.4, 26.8, 26.1, 25.9, 23.9, 18.0. ESI-HRMS calcd for m/z = 856.33940 $[M - PF_6]^+$, found m/z = 856.34062.

S4: A mixture of 2,6-diisopropylphenol (1.78 g, 10 mmol), 8-bromooctan-1-ol (2.2 g, 11 mmol) and K_2CO_3 (1.5 g, 11 mmol) was stirred at 80 °C in DMF (30 mL) overnight. After cooling to room temperature, the mixture was poured into H_2O (100 mL). The resulting mixture was extracted with CH_2Cl_2 (3 x 30 mL) and the combined organic phases were washed with saturated aqueous NaCl solution (100 mL). After drying ($MgSO_4$), the solvent was removed in vacuo to afford a crude precursor as a light-yellow oil. The crude precursor alcohol, *p*-toluenesulfonyl chloride (2.0 g, 10.5 mmol) and 4-dimethylaminopyridine (122 mg, 1 mmol) were stirred in Et_3N (5 mL) and CH_2Cl_2 (50 mL) at room temperature for 3 h. The solution was poured into H_2O (50 mL). The resulting mixture was extracted with CH_2Cl_2 (3 × 30 mL) and the combined organic phases were washed with saturated aqueous NaCl solution (50 mL). After drying ($MgSO_4$), the solvent was removed in vacuo and the resulting residue was purified by column chromatography (SiO_2: Hexanes / EtOAc 5:1) to afford **S4** (2.61 g, 57%). ^{1}H NMR (500 MHz, $CDCl_3$) δ 7.80 (d, J = 8.3 Hz, 2H), 7.35 (d, J = 8.3 Hz, 2H), 7.12 – 7.04 (m, 3H), 4.04 (t, J = 6.5 Hz, 2H), 3.71 (t, J = 6.6 Hz, 2H), 3.30 (hept, J = 6.9 Hz, 2H), 2.45 (s, 3H), 1.84 – 1.75 (m, 2H), 1.70 – 1.60 (m, 2H), 1.51 – 1.41 (m, 2H), 1.37 – 1.27 (m, 6H), 1.22 (d, J = 6.9 Hz, 12H). ^{13}C NMR (126 MHz, $CDCl_3$) δ 153.4, 144.6, 141.8, 133.3, 129.8, 127.9, 124.3, 123.9, 74.8, 70.6, 30.4, 29.3, 28.9, 28.8, 26.4, 26.0, 25.3, 24.1, 21.6. ESI-HRMS calcd for m/z = 460.26473 $[M + H]^+$, found m/z = 460.26455.

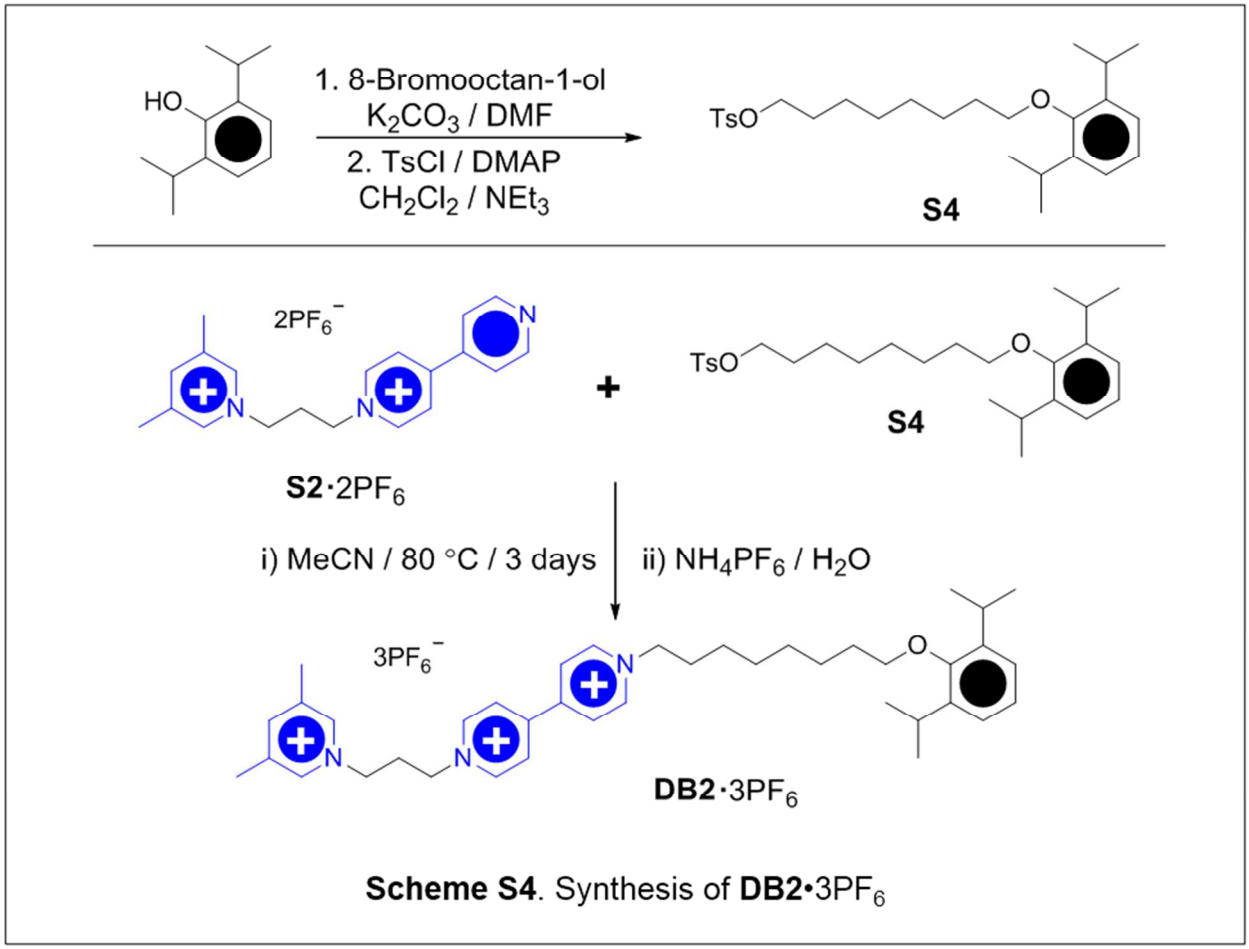

Scheme S4. Synthesis of **DB2**•3PF_6

DB2•3PF_6: A mixture of **S2**•2PF_6 (100 mg, 0.17 mmol) and **S4** (100 mg, 0.22 mmol) was stirred at 80 °C in MeCN (1 mL) for 3 days. After cooling to room temperature, the solvent was removed in vacuum. The resulting residue was purified by column chromatography ((SiO_2 : MeOH / NH_4Cl (aq, 2M) / $MeNO_2$ = 7:2:1), followed by counterion exchange (NH_4PF_6 / H_2O) to afford **DB2**•3PF_6 (131 mg, 76%). ^{1}H NMR (500 MHz, CD_3CN): δ 8.95 – 8.89 (m, 4H), 8.42 (d, *J* = 6.0 Hz, 2H), 8.41 – 8.36 (m, 4H), 8.20 (s, 1H), 7.15 – 7.03 (m, 3H), 4.71 (t, *J* = 7.5 Hz, 2H), 4.63 (t, *J* = 7.3 Hz, 2H), 4.56 (t, *J* = 7.5 Hz, 2H), 3.72 (t, *J* = 6.4 Hz, 2H), 3.30 (hept, *J* = 6.9 Hz, 2H), 2.73 – 2.58 (m, 2H), 2.50 (s, 6H), 2.09 – 1.98 (m, 2H), 1.85 – 1.74 (m, 2H), 1.57 – 1.48 (m, 2H), 1.46 – 1.38 (m, 6H), 1.19 (d, *J* = 6.9 Hz, 12H). ^{13}C NMR (126 MHz, CD_3CN): δ 153.0, 150.1, 149.3, 146.9, 145.5, 145.2, 141.4, 141.1, 139.1, 127.1, 126.9, 124.2, 123.6, 74.2, 61.8, 57.9, 57.3, 31.3, 30.7, 29.7, 28.6, 28.3, 25.8, 25.4, 25.2, 23.0, 17.1. ESI-HRMS calcd for *m/z* =

884.37070 $[M - PF_6]^+$, found *m/z* = 884.37143.

S5: A mixture of 2,6-diisopropylphenol (3.56 g, 20 mmol), 11-bromo-1-undecanol (5.1 g, 20 mmol) and K_2CO_3 (3 g, 22 mmol) was stirred at 80 °C in DMF (30 mL) overnight. After cooling to room temperature, the mixture was poured into H_2O (100 mL). The resulting mixture was extracted with CH_2Cl_2 (3 × 30 mL) and the combined organic phases were washed with saturated aqueous NaCl solution (100 mL). After drying ($MgSO_4$), the solvent was removed in vacuo to afford a crude precursor as a light-yellow oil. The crude precursor alcohol, *p*-toluenesulfonyl chloride (4.0 g, 21 mmol) and 4-dimethylaminopyridine (122 mg, 1 mmol) was stirred in Et_3N (10 mL) and CH_2Cl_2 (50 mL) at room temperature for 3 h. The solution was poured into H_2O (50 mL). The resulting mixture was extracted with CH_2Cl_2 (3 × 30 mL) and the combined organic phases were washed with saturated aqueous NaCl solution (50 mL). After drying ($MgSO_4$), the solvent was removed in vacuo and the resulting residue was purified by column chromatography (SiO_2: Hexanes / EtOAc 5:1) to afford **S5** (6.94 g, 69%). ^{1}H NMR (500 MHz, $CDCl_3$) ^{1}H NMR (500 MHz, $CDCl_3$) δ 7.79 (d, *J* = 8.3 Hz, 2H), 7.34 (d, *J* = 8.0 Hz, 2H), 7.12 – 7.04 (m, 3H), 4.02 (t, *J* = 6.5 Hz, 2H), 3.72 (t, *J* = 6.6 Hz, 2H), 3.31 (hept, *J* = 6.9 Hz, 2H), 2.45 (s, 3H), 1.87 – 1.75 (m, 2H), 1.67 – 1.59 (m, 2H), 1.53 – 1.44 (m, 2H), 1.40 – 1.24 (m, 12H), 1.22 (d, *J* = 7.1 Hz, 12H). ^{13}C NMR (126 MHz, $CDCl_3$) δ 153.5, 144.6, 141.8, 133.3, 129.8, 127.9, 124.3, 123.9, 74.9, 70.7, 30.4, 29.6, 29.5, 29.5, 29.4, 29.0, 28.9, 26.4, 26.1, 25.4, 24.1, 21.7. ESI-HRMS calcd for *m/z* = 502.31168 $[M + H]^+$, found *m/z* = 502.31180.

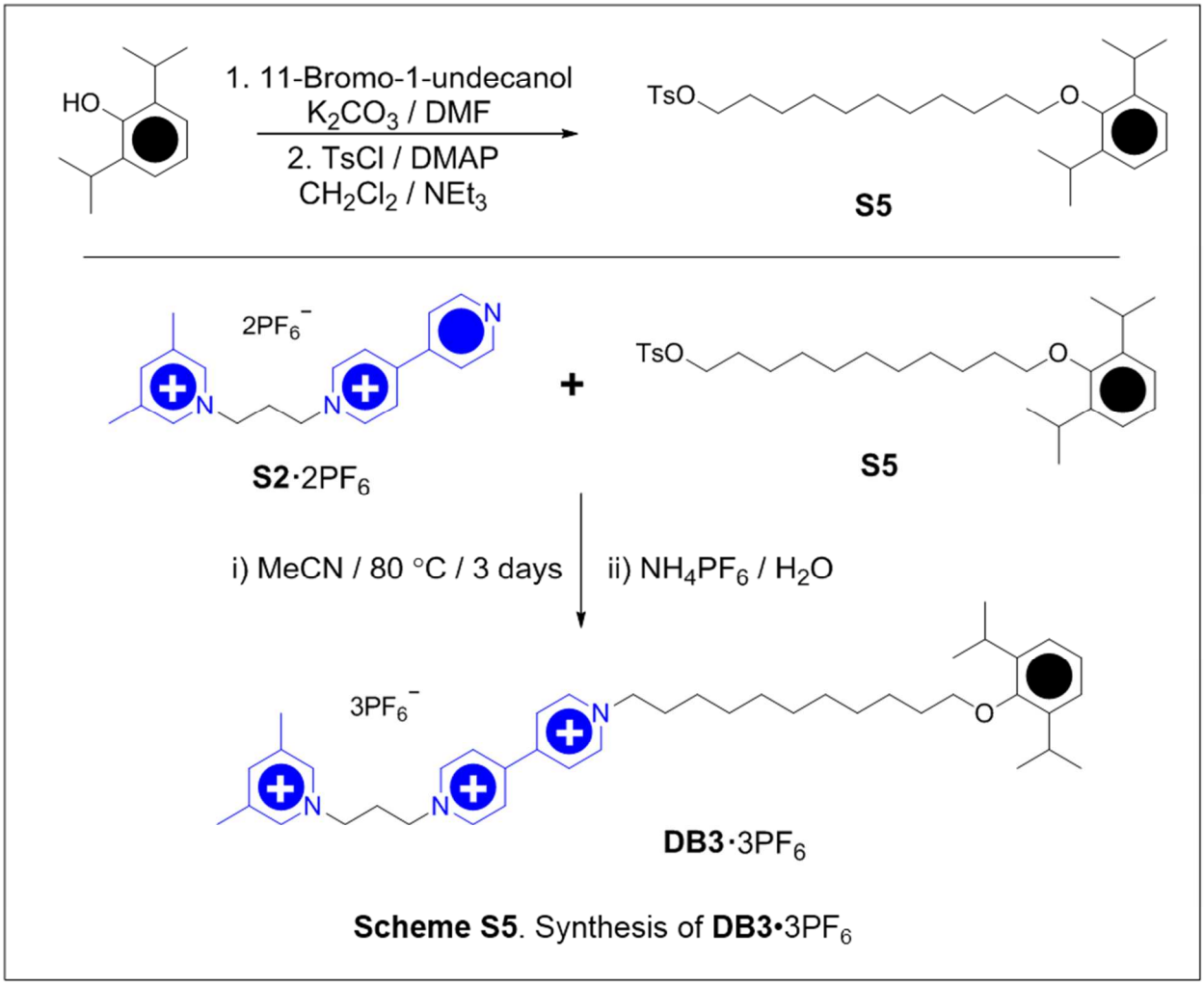

Scheme S5. Synthesis of **DB3**•3PF_6

DB3•3PF_6: A mixture of **S2**•2PF_6 (100 mg, 0.17 mmol) and **S5** (100 mg, 0.20 mmol) was stirred at 80 °C in MeCN (1 mL) for 3 days. After cooling to room temperature, the solvent was removed under reduced pressure. The resulting residue was purified by column chromatography (SiO_2 : MeOH / NH_4Cl (aq, 2M) / $MeNO_2$ = 7:2:1), followed by counterion exchange (NH_4PF_6 / H_2O) to afford **DB3**•3PF_6 (61 mg, 34%). ^{1}H NMR (500 MHz, CD_3CN): δ 8.95 (d, *J* = 5.4 Hz, 2H), 8.93 (d, *J* = 6.9 Hz, 2H), 8.45 (d, *J* = 6.9 Hz, 2H), 8.43 (s, 2H), 8.41 (d, *J* = 6.4 Hz, 2H), 8.23 (s, 1H), 7.17 – 7.06 (m, 3H), 4.73 (t, *J* = 8.0 Hz, 2H), 4.64 (t, *J* = 7.6 Hz, 2H), 4.59 (t, *J* = 7.5 Hz, 2H), 3.74 (t, *J* = 6.4 Hz, 2H), 3.34 (hept, *J* = 6.9 Hz, 2H), 2.75 – 2.62 (m, 2H), 2.53 (s, 6H), 2.09 – 2.00 (m, 2H), 1.88 – 1.76 (m, 2H), 1.54 (p, *J* = 6.8 Hz, 2H), 1.46 – 1.34 (m, 12H),

1.22 (d, J = 6.9 Hz, 12H). ^{13}C NMR (126 MHz, CD_3CN): δ 153.0, 150.1, 149.3, 146.9, 145.5, 145.2, 141.4, 141.1, 139.1, 127.1, 126.8, 124.1, 123.6, 74.2, 61.8, 57.9, 57.3, 31.3, 30.7, 29.7, 29.0, 28.9, 28.8, 28.7, 28.3, 25.8, 25.4, 25.2, 23.0, 17.1. ESI-HRMS calcd for m/z = 926.41765 $[M - PF_6]^+$, found m/z = 926.41847.

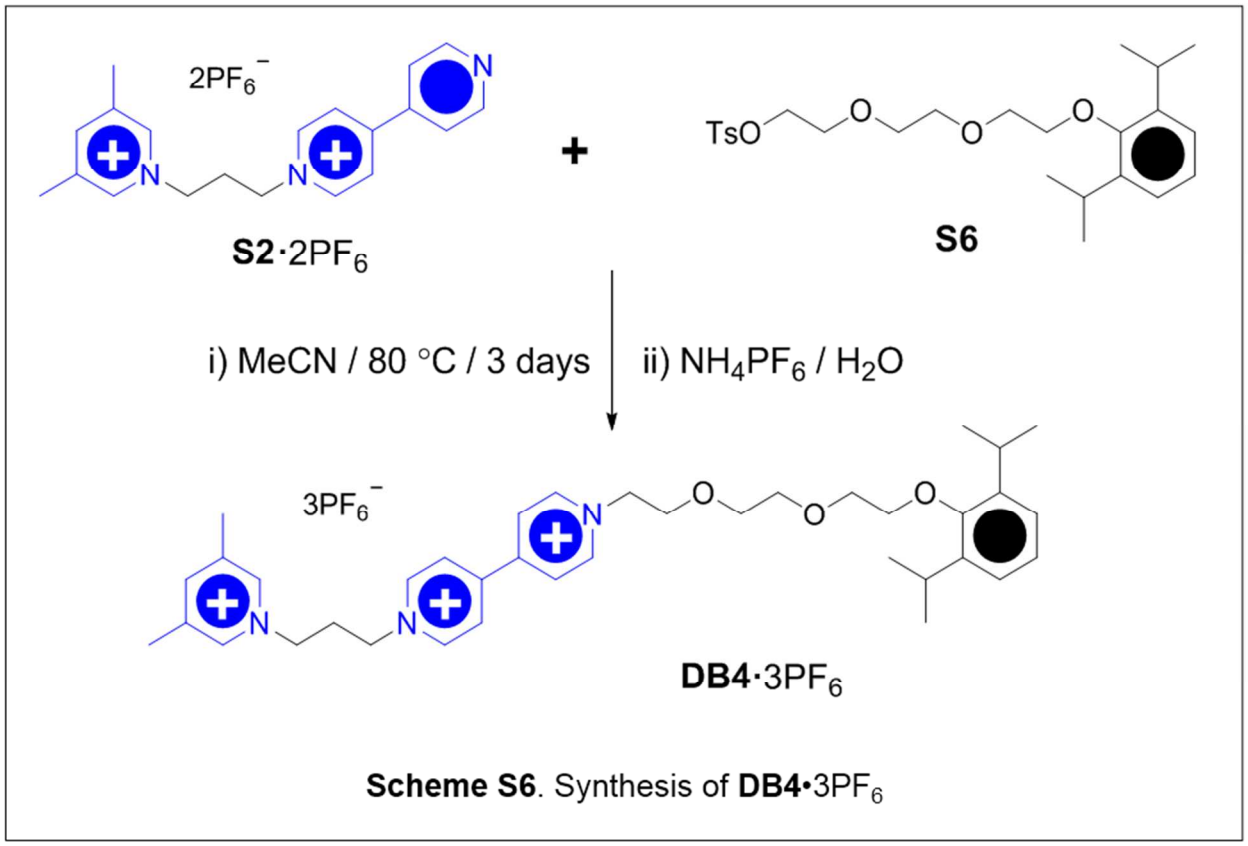

Scheme S6. Synthesis of **DB4**•3PF_6

DB4•3PF_6: A mixture of **S2**•2PF_6 (100 mg, 0.17 mmol) and **S6**[2] (100 mg, 0.22 mmol) was stirred at 80 °C in MeCN (1 mL) for 3 days. After cooling to room temperature, the solvent was removed under reduced pressure. The resulting residue was purified by column chromatography (SiO_2 : MeOH / NH_4Cl (aq, 2M) / $MeNO_2$ = 7:2:1), followed by counterion exchange (NH_4PF_6 / H_2O) to afford **DB4**•3PF_6 (101 mg, 58%). ^{1}H NMR (500 MHz, CD_3CN): δ 8.99 (d, J = 6.9 Hz, 2H), 8.86 (d, J = 6.4 Hz, 2H), 8.39 (s, 2H), 8.34 (d, J = 6.5 Hz, 2H), 8.29 (d, J = 6.3 Hz, 2H), 8.20 (s, 1H), 7.17 – 7.06 (m, 3H), 4.80 (t, J = 4.8 Hz, 2H), 4.69 (t, J = 7.6 Hz, 2H), 4.55 (t, J =

7.5 Hz, 2H), 4.03 (t, J = 4.3 Hz, 2H), 3.90 – 3.86 (m, 2H), 3.80 – 3.76 (m, 2H), 3.74 – 3.70 (m, 2H), 3.69 – 3.64 (m, 2H), 3.37 (hept, J = 6.9 Hz, 2H), 2.69 – 2.60 (m, 2H), 2.50 (s, 6H), 1.15 (d, J = 6.9 Hz, 12H). ^{13}C NMR (126 MHz, CD_3CN): δ 153.5, 151.0, 150.4, 147.8, 146.9, 146.3, 142.4, 142.0, 140.0, 128.0, 127.3, 125.4, 124.8, 74.4, 70.9, 70.7, 69.2, 62.2, 58.9, 58.2, 32.3, 26.5, 23.9, 18.0. ESI-HRMS calcd for m/z = 888.32923 $[M - PF_6]^+$, found m/z = 888.32947.

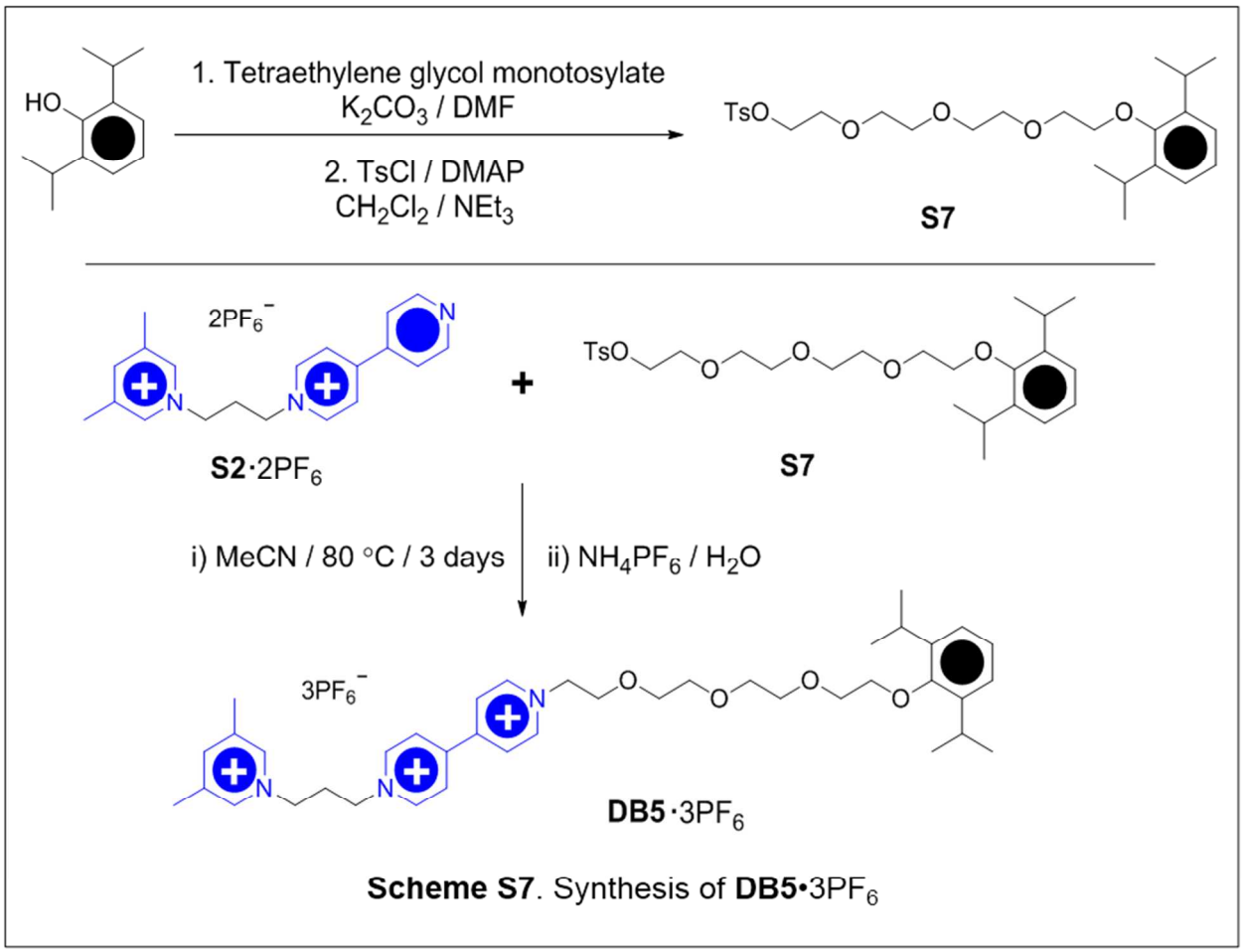

Scheme S7. Synthesis of **DB5**•3PF_6

S7: A mixture of 2,6-diisopropylphenol (0.52 g, 2.9 mmol), tetraethylene glycol monotosylate (1.0 g, 2.9 mmol) and K_2CO_3 (0.7 g, 5 mmol) was stirred at 80 °C in DMF (20 mL) overnight. After cooling to room temperature, the mixture was poured into H_2O (100 mL). The resulting mixture was extracted with CH_2Cl_2 (3 × 30 mL) and the combined organic phases were washed

with saturated aqueous NaCl solution (100 mL). After drying ($MgSO_4$), the solvent was removed in vacuo to afford the crude alcohol as a light-yellow oil. This crude precursor alcohol, *p*-toluenesulfonyl chloride (0.57 g, 3 mmol) and 4-dimethylaminopyridine (20 mg, 0.16 mmol) were stirred in Et_3N (5 mL) and CH_2Cl_2 (30 mL) at room temperature for 3 h. The solution was poured into H_2O (50 mL). The resulting mixture was extracted with CH_2Cl_2 (3 × 30 mL) and the combined organic phases were washed with saturated aqueous NaCl solution (50 mL). After drying ($MgSO_4$), the solvent was removed in vacuo and the resulting residue was purified by column chromatography (SiO_2: Hexanes / EtOAc 1:1) to afford **S7** (0.58 g, 40%). ^{1}H NMR (500 MHz, $CDCl_3$) δ 7.80 (d, *J* = 8.3 Hz, 2H), 7.33 (d, *J* = 8.1 Hz, 2H), 7.09 (s, 3H), 4.16 (t, *J* = 5.0 Hz, 2H), 3.93 – 3.89 (m, 2H), 3.87 – 3.82 (m, 2H), 3.77 – 3.72 (m, 2H), 3.72 – 3.67 (m, 4H), 3.66 – 3.62 (m, 2H), 3.62 – 3.58 (m, 2H), 3.37 (hept, *J* = 6.9 Hz, 2H), 2.44 (s, 3H), 1.21 (d, *J* = 6.9 Hz, 12H). ^{13}C NMR (126 MHz, $CDCl_3$) δ 153.0, 144.8, 141.8, 132.9, 129.8, 128.0, 124.6, 124.0, 73.8, 71.0, 70.8, 70.8, 70.7, 70.6, 69.2, 68.7, 26.2, 24.2, 21.7. ESI-HRMS calcd for *m/z* = 508.24947 $[M + H]^+$, found *m/z* = 508.25053.

DB5•$3PF_6$: A mixture of **S2•**$2PF_6$ (100 mg, 0.17 mmol) and **S7** (150 mg, 0.29 mmol) was stirred at 80 °C in MeCN (1 mL) for 3 days. After cooling to room temperature, the solvent was removed under reduced pressure. The resulting residue was purified by column chromatography (SiO_2 : MeOH / NH_4Cl (aq, 2M) / $MeNO_2$ = 7:2:1), followed by counterion exchange (NH_4PF_6 / H_2O) to afford **DB5•**$3PF_6$ (39 mg, 21%). ^{1}H NMR (500 MHz, CD_3CN): δ 9.00 (d, *J* = 7.0 Hz, 2H), 8.91 (d, *J* = 6.7 Hz, 2H), 8.44 (d, *J* = 7.0 Hz, 2H), 8.43 – 8.39 (m, 4H), 8.24 (s, 1H), 7.18 – 7.07 (m, 3H), 4.81 (t, *J* = 5.9 Hz, 2H), 4.71 (t, *J* = 7.6 Hz, 2H), 4.58 (t, *J* = 7.5 Hz, 2H), 4.03 (t, *J* = 5.0 Hz, 2H), 3.91 – 3.87 (m, 2H), 3.83 – 3.79 (m, 2H), 3.73 – 3.67 (m, 4H), 3.67 – 3.60 (m, 4H), 3.39 (hept, *J* = 6.9 Hz, 2H), 2.72 – 2.62 (m, 2H), 2.53 (s, 6H), 1.19 (d, *J* = 6.9 Hz, 12H). ^{13}C NMR (126 MHz, CD_3CN): δ 152.6, 150.2, 149.5, 146.9, 146.0, 145.4, 141.5, 141.1, 139.1, 127.1,

126.4, 124.5, 123.8, 73.6, 70.1, 70.0, 69.8, 69.8, 69.7, 68.2, 61.3, 57.9, 57.3, 31.3, 25.6, 23.0, 17.1. ESI-HRMS calcd for m/z = 932.35544 $[M - PF_6]^+$, found m/z = 932.35600.

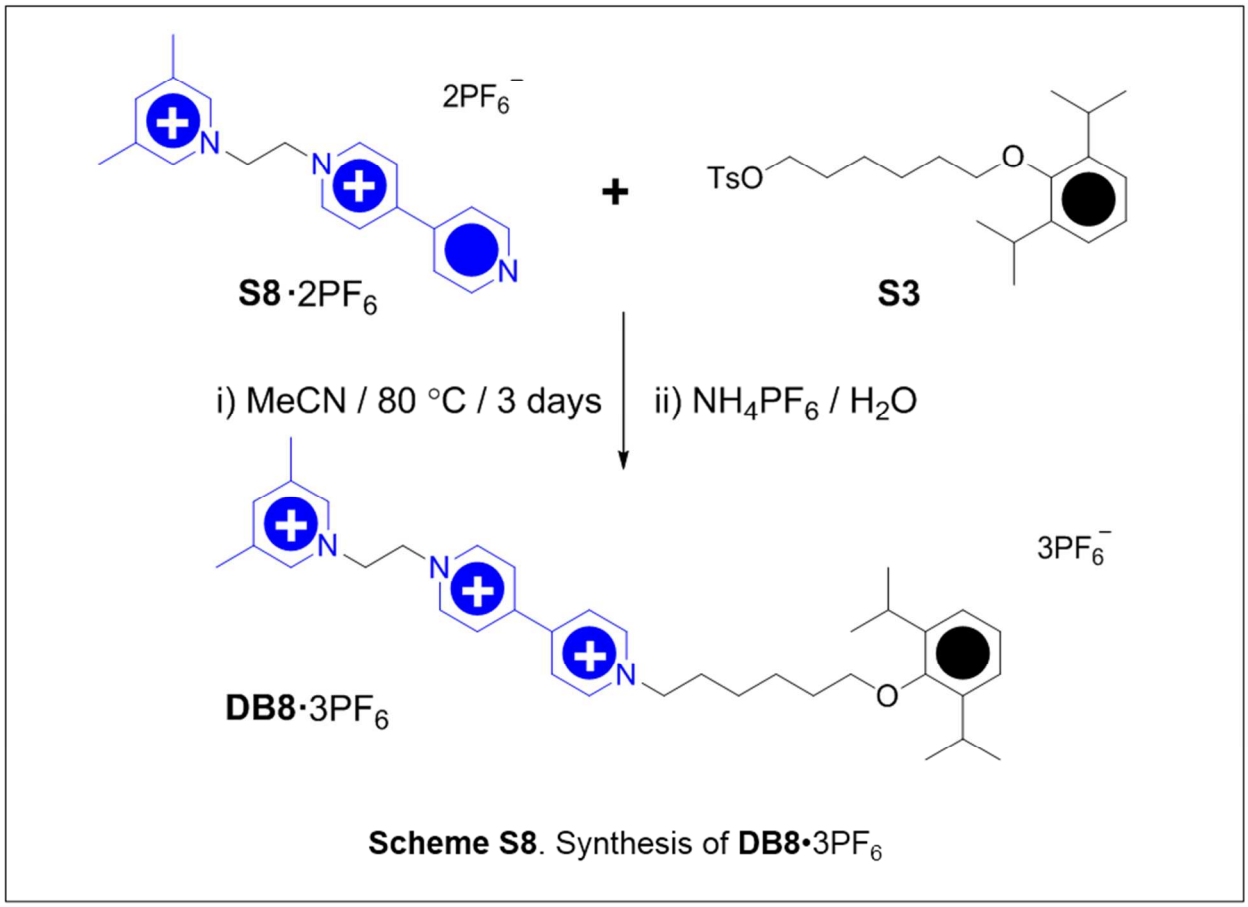

Scheme S8. Synthesis of **DB8**•3PF_6

DB8•3PF_6: A mixture of **S8**•2PF_6[3] (100 mg, 0.17 mmol) and **S3** (100 mg, 0.23 mmol) was stirred at 80 °C in MeCN (1 mL) for 3 days. After cooling to room temperature, the solvent was removed under reduced pressure. The resulting residue was purified by column chromatography (SiO_2 : MeOH / NH_4Cl (aq, 2M) / $MeNO_2$ = 7:2:1), followed by counterion exchange (NH_4PF_6 / H_2O) to afford **DB8**•3PF_6 (100 mg, 60%). ^{1}H NMR (500 MHz, CD_3CN): δ 8.96 (d, J = 6.9 Hz, 2H), 8.90 (d, J = 6.9 Hz, 2H), 8.47 (d, J = 6.9 Hz, 2H), 8.45 – 8.40 (m, 4H), 8.30 (s, 1H), 7.18 – 7.07 (m, 3H), 5.20 (t, J = 6.6 Hz, 2H), 5.05 (t, J = 6.6 Hz, 2H), 4.68 (t, J = 7.5 Hz, 2H), 3.76 (t, J = 6.4 Hz, 2H), 3.33 (hept, J = 6.9 Hz, 2H), 2.52 (s, 6H), 2.15 – 2.07 (m, 2H), 1.89 – 1.79 (m, 2H),

1.68 – 1.59 (m, 2H), 1.56 – 1.48 (m, 2H), 1.22 (d, J = 6.9 Hz, 12H). ^{13}C NMR (126 MHz, CD_3CN): δ 154.3, 152.4, 150.5, 149.4, 147.2, 146.7, 142.8, 142.8, 141.0, 128.9, 128.3, 125.6, 125.0, 75.4, 63.2, 60.9, 60.3, 31.9, 30.8, 27.2, 26.6, 26.3, 24.3, 18.4. ESI-HRMS calcd for m/z = 842.32375 $[M - PF_6]^+$, found m/z = 842.32450.

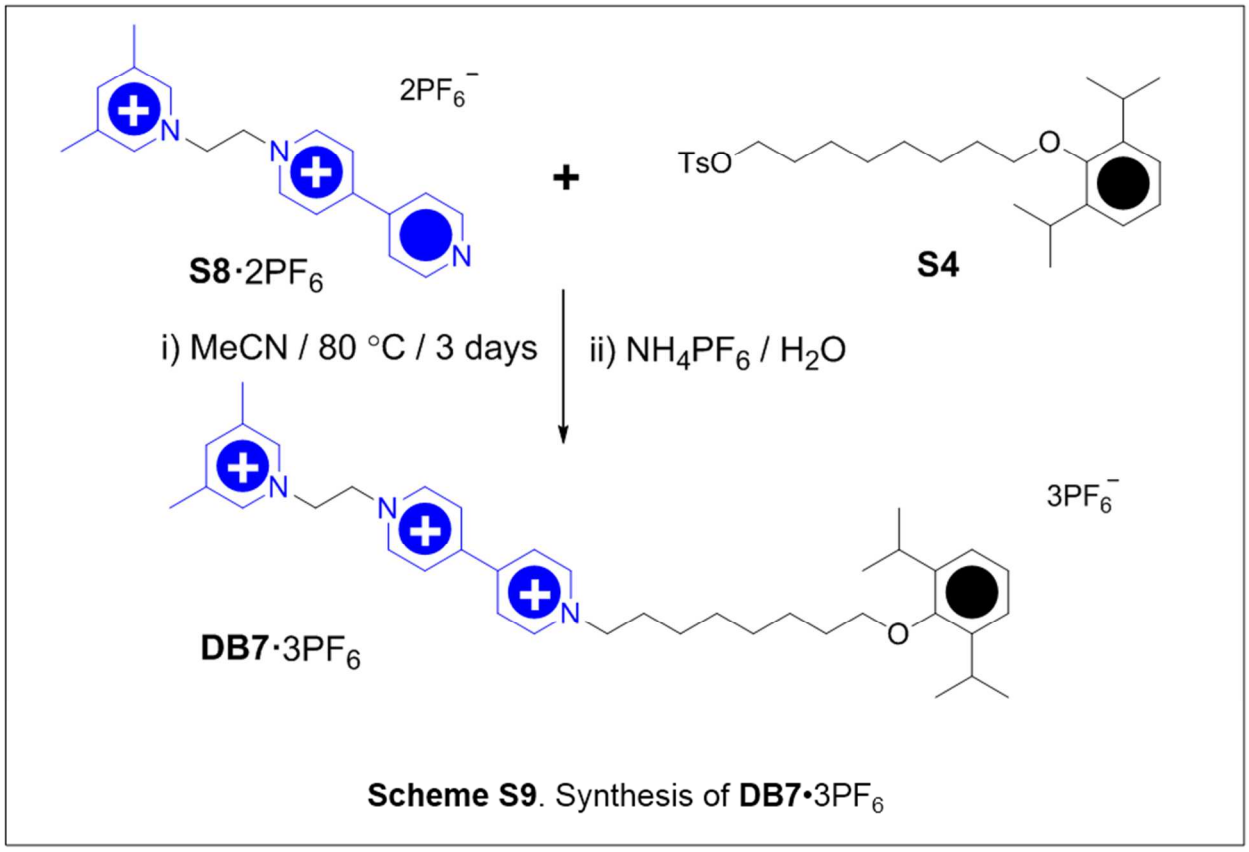

Scheme S9. Synthesis of **DB7**•3PF_6

DB7•3PF_6: A mixture of **S8**•2PF_6[3] (100 mg, 0.17 mmol) and **S4** (100 mg, 0.22 mmol) was stirred at 80 °C in MeCN (1 mL) for 3 days. After cooling to room temperature, the solvent was removed under reduced pressure. The resulting residue was purified by column chromatography (SiO_2 : MeOH / NH_4Cl (aq, 2M) / $MeNO_2$ = 7:2:1), followed by counterion exchange (NH_4PF_6 / H_2O) to afford **DB7**•3PF_6 (118 mg, 67%). ^{1}H NMR (500 MHz, CD_3CN): δ 8.92 (d, J = 6.3 Hz, 2H), 8.82 (d, J = 6.6 Hz, 2H), 8.44 (d, J = 6.4 Hz, 2H), 8.39 (d, J = 6.3 Hz, 2H), 8.36 (s, 2H), 8.27 (s, 1H), 7.16 – 7.03 (m, 3H), 5.16 (t, J = 6.5 Hz, 2H), 5.01 (t, J = 6.5 Hz, 2H), 4.64 (t, J =

7.6 Hz, 2H), 3.73 (t, J = 6.4 Hz, 2H), 3.31 (hept, J = 6.9 Hz, 2H), 2.49 (s, 6H), 2.09 – 2.01 (m, 2H), 1.84 – 1.77 (m, 2H), 1.59 – 1.49 (m, 2H), 1.47 – 1.39 (m, 6H), 1.19 (d, J = 6.9 Hz, 12H). ^{13}C NMR (126 MHz, CD_3CN): δ 154.4, 152.4, 150.5, 149.5, 147.1, 146.7, 142.8, 142.7, 141.0, 128.9, 128.3, 125.5, 125.0, 75.6, 63.2, 60.9, 60.4, 32.0, 31.0, 29.9, 29.6, 27.2, 26.7, 26.6, 24.3, 18.4. ESI-HRMS calcd for m/z = 870.35505 $[M - PF_6]^+$, found m/z = 870.35505.

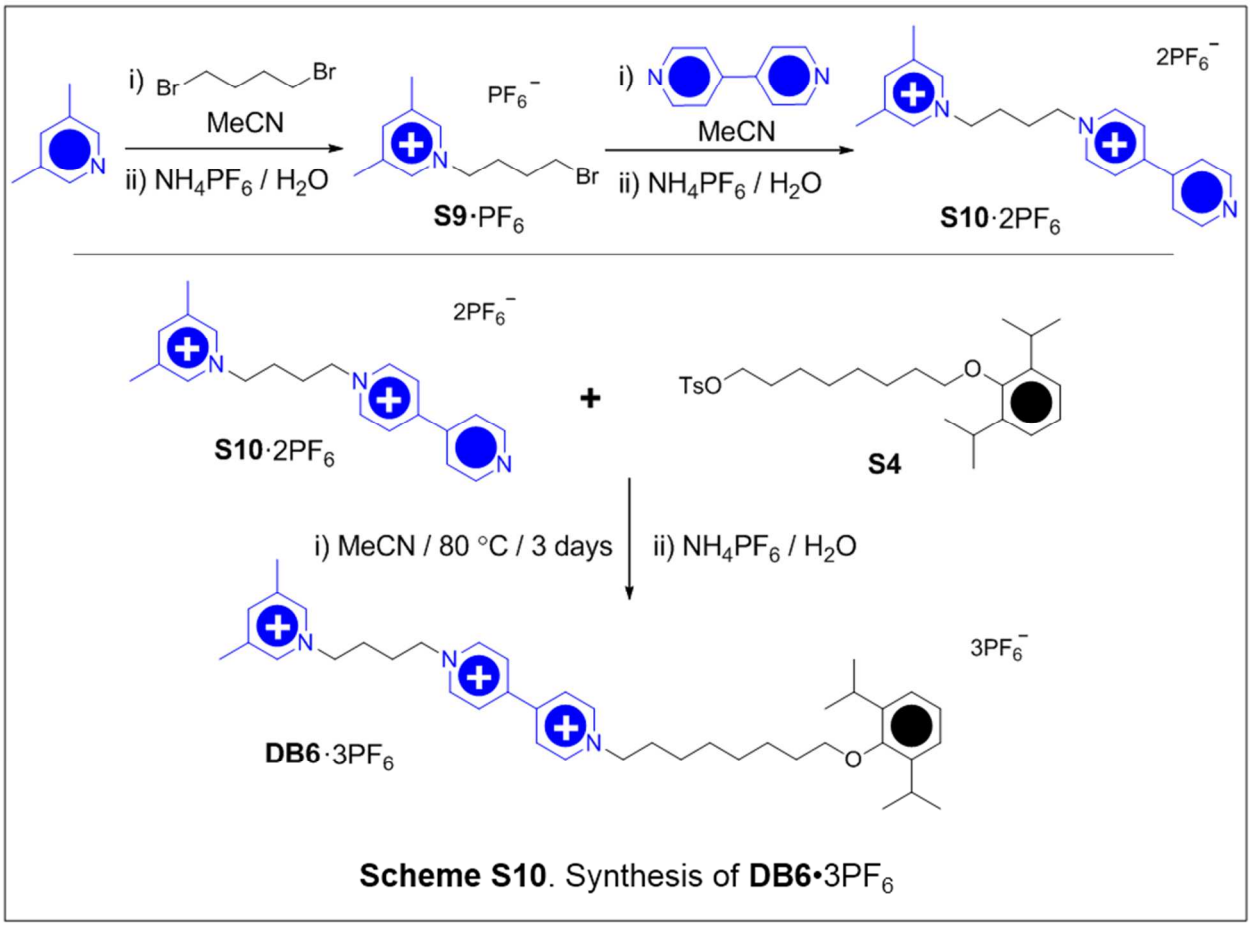

Scheme S10. Synthesis of **DB6**•3PF_6

S10•2PF_6: A mixture of 3,5-lutidine (1.07 g, 10 mmol) and 1,4-dibromobutane (10 mL) was stirred at 120 °C overnight. After cooling to room temperature, the mixture was poured into Et_2O (50 mL). The resulting suspension was extract with H_2O (3 × 20 mL), then NH_4PF_6 (2 g) was added to the combined water phase. The precipitate was filtered and washed with H_2O (3 × 5 mL) to afford **S9**•PF_6 (3.45 g, 89%). A mixture of **S9**•PF_6 (3.0 g, 7.7 mmol) and 4,4′-bipyridine (1.0 g,

6.4 mmol) were stirred in MeCN (10 mL) for 3 days. After cooling to room temperature, the mixture was poured into Et_2O (50 mL). The resulting suspension was filtered and washed with Et_2O (3 × 5 mL). The solid was dissolved in H_2O (50 mL), then NH_4PF_6 (2 g) was added. The precipitate was filtered and washed with H_2O (3 × 5 mL) to afford a crude product, which was purified by column chromatography (SiO_2 : MeOH / NH_4Cl (aq, 2M) / $MeNO_2$ = 7:2:1), followed by counterion exchange (NH_4PF_6 / H_2O) to afford **S10**•2PF_6 (2.07 g, 54%) as a white solid. ^{1}H NMR (500 MHz, CD_3CN): δ 8.91 – 8.86 (m, 2H), 8.77 (d, *J* = 6.9 Hz, 2H), 8.39 – 8.33 (m, 4H), 8.18 (d, *J* = 5.6 Hz, 1H), 7.82 (d, *J* = 6.2 Hz, 2H), 4.59 (t, *J* = 5.8 Hz, 2H), 4.47 (t, *J* = 5.9 Hz, 2H), 2.49 (s, 6H), 2.07 – 2.01 (m, 4H). ^{13}C NMR (126 MHz, CD_3CN): δ 154.0, 150.8, 146.5, 144.6, 140.9, 140.8, 138.8, 125.7, 121.4, 60.1 (2×C), 26.9, 26.7, 17.0. ESI-HRMS calcd for *m/z* = 464.16903 $[M - PF_6]^+$, found *m/z* = 464.16962.

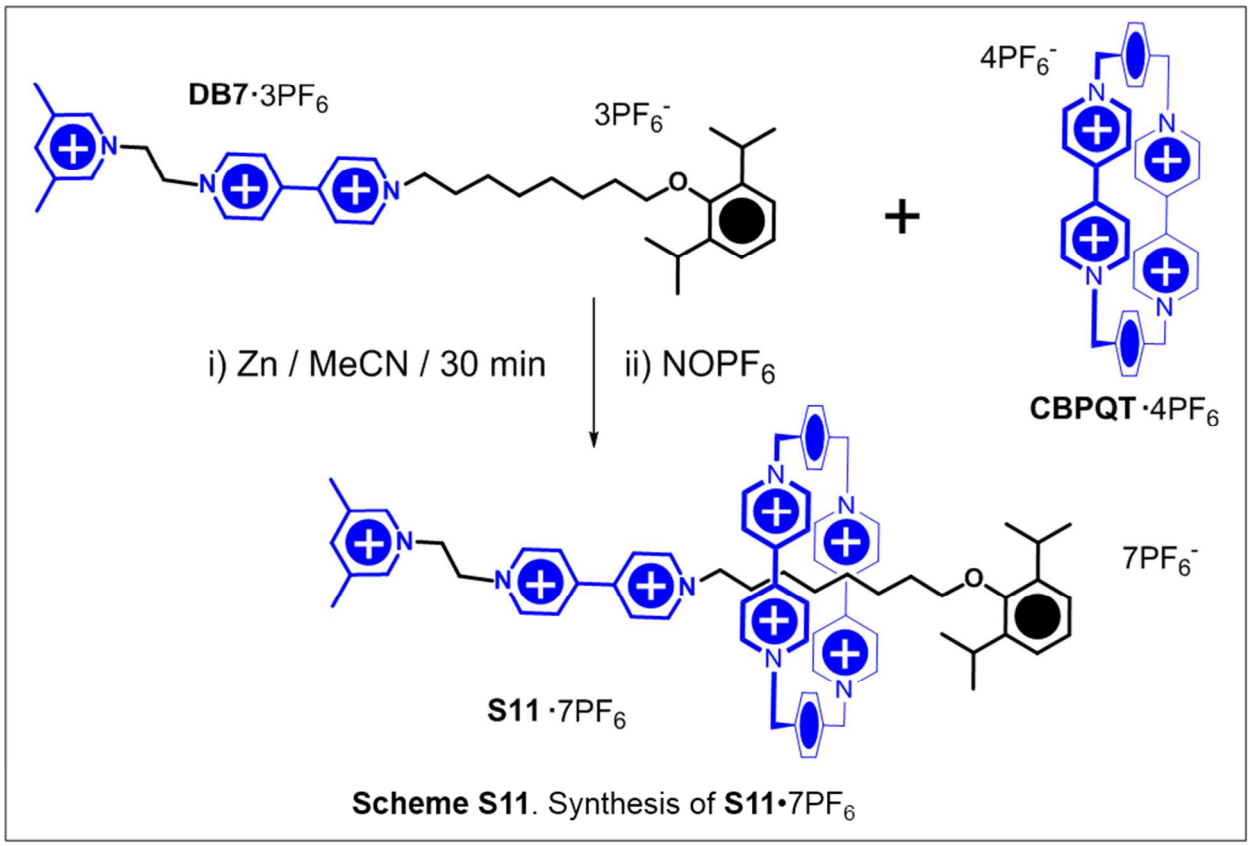

Scheme S11. Synthesis of **S11**•7PF_6

DB6•3PF_6: A mixture of **S18**•2PF_6 (100 mg, 0.17 mmol) and **S4** (100 mg, 0.22 mmol) was stirred at 80 °C in MeCN (1 mL) for 3 days. After cooling to room temperature, the solvent was removed under reduced pressure. The resulting residue was purified by column chromatography (SiO_2 : MeOH / NH_4Cl (aq, 2M) / $MeNO_2$ = 7:2:1), followed by counterion exchange (NH_4PF_6 / H_2O) to afford **DB6**•3PF_6 (154 mg, 90%). ^{1}H NMR (500 MHz, CD_3CN): δ 8.93 (d, *J* = 7.0 Hz, 2H), 8.91 (d, *J* = 6.9 Hz, 2H), 8.44 – 8.39 (m, 4H), 8.38 (s, 2H), 8.19 (t, *J* = 6.5 Hz, 1H), 7.18 – 7.08 (m, 3H), 4.73 – 4.60 (m, 4H), 4.49 (t, *J* = 6.5 Hz,2H), 3.75 (t, *J* = 6.4 Hz, 2H), 3.33 (hept, *J* = 6.9 Hz, 2H), 2.50 (s, 6H), 2.12 – 2.02 (m, 6H), 1.88 – 1.76 (m, 2H), 1.59 – 1.53 (m, 2H), 1.48 – 1.43 (m, 6H), 1.22 (d, *J* = 6.9 Hz, 12H). ^{13}C NMR (126 MHz, CD_3CN): δ 153.0, 149.8, 149.4, 146.5, 145.3, 145.2, 141.4, 141.0, 138.8, 126.9, 126.8, 124.2, 123.6, 74.2, 61.8, 60.7, 60.0, 30.7, 29.7, 28.6, 28.3, 27.0, 26.7, 25.8, 25.4, 25.2, 23.0, 17.0. ESI-HRMS calcd for *m/z* = 898.38635 $[M - PF_6]^+$, found *m/z* = 898.38755.

S11•7PF_6: **DB7**•3PF_6 (30 mg, 0.03 mmol) and **CBPQT**•4PF_6 (35 mg, 0.033 mmol) were dissolved in MeCN (20 mL, degassed). An excess of activated Zn dust was added to the solution in a glovebox. After stirring for 30 min, the mixture was filtered and $NOPF_6$ (20 mg, 0.11 mmol) was added. The mixture was analyzed by HPLC-MS before being purified by column chromatography (C_{18}-functionalized SiO_2: H_2O / MeCN with 0.1% CF_3COOH). The product containing fractions were combined, an excess of NH_4PF_6 was added and the organic solvent was evaporated under reduced pressure. The resulting precipitate was collected by filtration, washed with copious amounts H_2O, and dried under high vacuum to afford **S11**•7PF_6 (30 mg, 50%) as a colorless solid. ^{1}H NMR (500 MHz, CD_3CN): δ 9.17 – 8.99 (m, 10H), 8.86 (d, *J* = 6.3 Hz, 2H), 8.57 – 8.55 (m, 4H), 8.44 (b, 8H), 8.38 (s, 2H), 8.29 (s, 1H), 7.62 (s, 8H), 7.33 – 7.16 (m, 3H),

5.84 (dd, J = 22.7, 13.8 Hz, 8H), 5.20 (t, J = 6.4 Hz, 2H), 5.04 (t, J = 6.6 Hz, 2H), 4.63 (t, J = 8.0 Hz, 2H), 3.01 – 2.96 (m, 4H), 2.51 (s, 6H), 1.67 – 1.57 (m, 2H), 1.47 (d, J = 7.0 Hz, 12H), 0.57 (b, 2H), –1.24 (b, 2H), –1.45 (b, 2H), –1.68 (b, 4H). ^{13}C NMR (126 MHz, CD_3CN): δ 153.0, 152.1, 150.2, 149.1, 148.7, 146.8, 146.3 (2×C), 142.3, 141.8, 140.7, 136.8, 131.0, 128.6, 128.0, 127.8, 126.0, 125.2, 74.8, 65.3, 62.4, 60.6, 60.0, 31.6, 30.4, 29.8, 29.6, 26.9 (2×C), 26.5, 24.5, 18.0. ESI-HRMS calcd for m/z = 912.75460 $[M - 2PF_6]^{2+}$, found m/z = 912.75481.

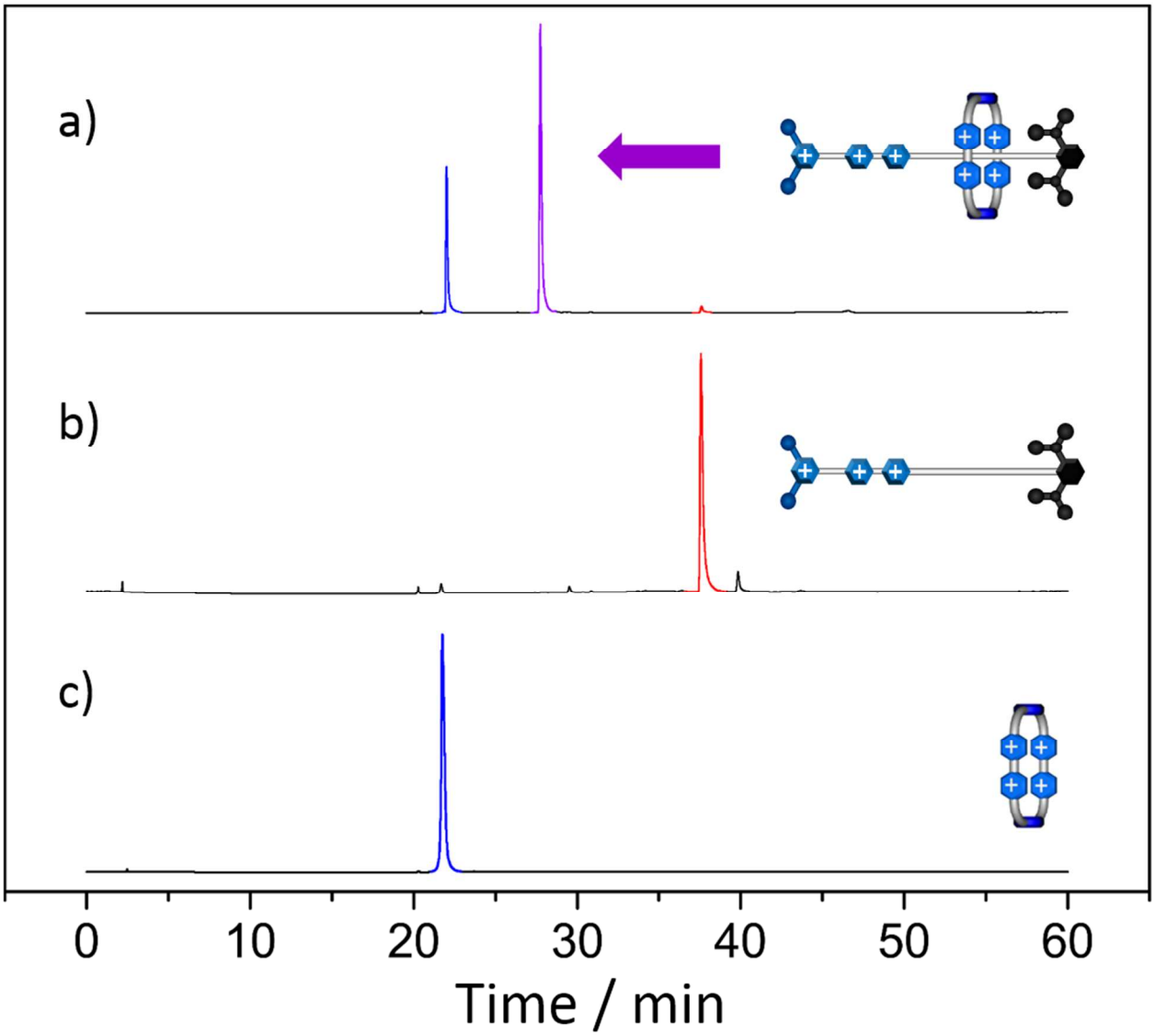

Figure S1. Analytical HPLC trace of a) **DB7**•3PF_6 and **CBPQT**•4PF_6 immediately after the reduction and oxidation procedure, b) **DB7**•3PF_6 and c) **CBPQT**•4PF_6

3. UV/Vis/NIR Spectroscopy

DB0•4PF_6 (1.0 mg, 0.001 mmol) or **CBPQT**•4PF_6 (1.1 mg, 0.001 mmol) was dissolved in MeCN (10 mL, degassed). Excess of activated Zn dust was added to it and stirred for 10 min in a glovebox. The solution changed to blue in seconds. The UV/Vis/NIR spectrum was recorded after filtering. A mixture of **DB0**•4PF_6 (1.0 mg, 0.001 mmol) and **CBPQT**•4PF_6 (1.1 mg, 0.001 mmol) was dissolved in MeCN (10 mL, degassed). Excess of activated Zn dust was added to the mixture and it was stirred for 10 min in a glovebox. The solution changed to blue then purple in seconds. The UV/Vis/NIR spectrum was recorded after filtering.

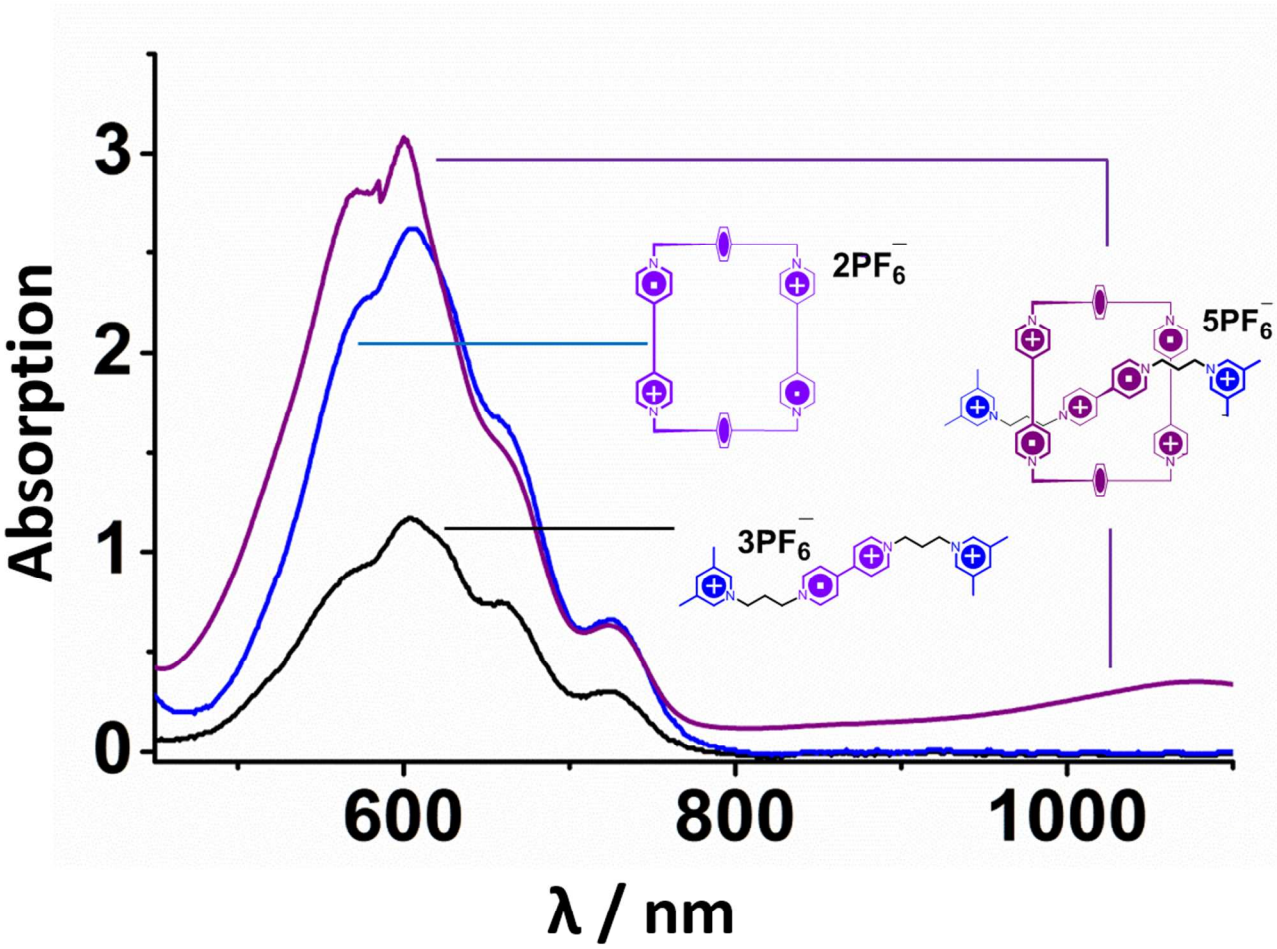

Figure S2. UV/Vis/NIR Spectra of **DB0**$^{3+\bullet}$ (black trace), **CBPQT**$^{2(+\bullet)}$ (blue trace), **DB0**$^{3+\bullet}$⊂**CBPQT**$^{2(+\bullet)}$ (purple trace). The broad peak around 1100 nm indicates formation of a trisradical complex[4]. [**CBPQT**$^{4+}$] = 1.0 × 10^{-4} M. [**DB0**$^{4+}$] = 1.0 × 10^{-4} M.

4. Single Crystal X-Ray Diffraction

Excess of activated zinc dust was added to a mixture of **DB0**•4PF_6 (1.0 mg, 1.0 μmol) and **CBPQT**•4PF_6 (1.1 mg, 1.0 μmol) in MeCN (1 mL) in a glovebox, and the mixture was stirred for 30 min. After filtering, the purple solution was kept under an atmosphere of iPr_2O at 0 °C to allow slow vapor diffusion to occur. Single crystals of **DB0⊂CBPQT**•6PF_6, an overall bisradical species, were formed after a month. They were immersed in inert oil and transferred to the cold gas stream of a Bruker Kappa APEX CCD area detector, equipped with a CuKα microsource with MX optics. A SADABS-2008/1 (Bruker,2008) was used for absorption correction. *wR*2(int) was 0.0952 before and 0.0331 after correction. The ratio of minimum to maximum transmission was 0.8222. The λ/2 correction factor is not present.

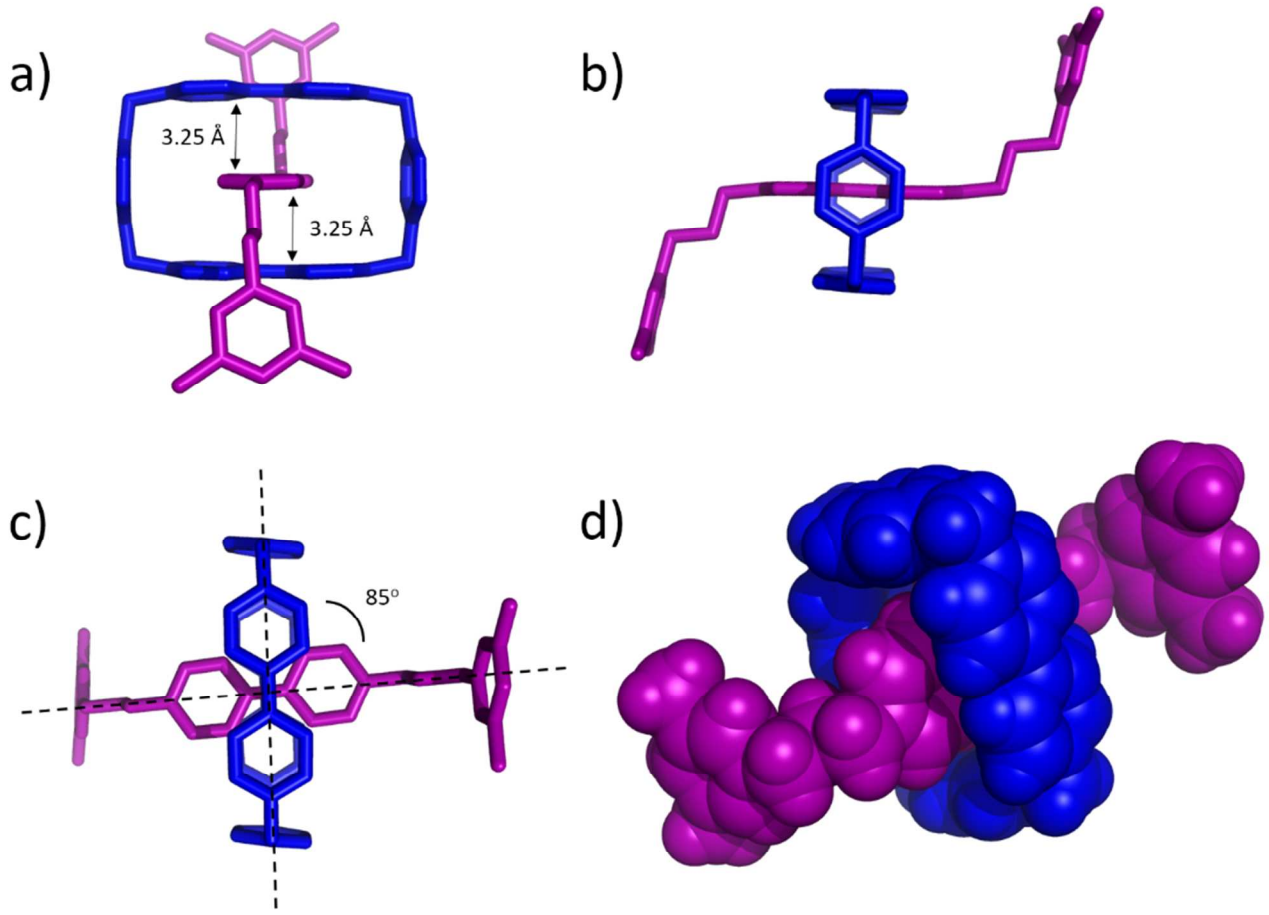

Figure S3. Crystal structure of **DB0⊂CBPQT**•6PF_6 a) top view, b) and c) side views, d) space filling representation. Solvent molecules and counter ions are omitted for clarity.

Crystal Data for $C_{82}H_{94}F_{36}N_{16}P_6$, M =2173.55, monoclinic, a = 18.8758(10), b = 20.3394(13), c = 13.1067(8), β = 104.883(3)°, V = 4863.1(5) Å^3, T = 99.98, space group *P21/c* (no. 14), Z = 2, μ(CuKα) = 2.114, 30255 reflections measured, 8210 unique (R_{int} = 0.0327) which were used in all calculations. The final $wR(F_2)$ was 0.1898 (all data), R_1 = 0.0696 for $I > 2\sigma(I)$. No special refinement necessary. Crystallographic data (excluding structure factors) for the structures reported in this communication have been deposited with the Cambridge Crystallographic Data Center as supplementary publication no. CCDC–1019889.

It is worth highlighting that the solid-state structures contains 6 hexafluorophosphate anions, indicating the inclusion complex is not a trisradical complex as we observed by UV/Vis/NIR spectroscopy in solution. Possible reasons for this unexpected phenomenon might be that: (i) the trace amount of oxygen in glovebox (< 10 ppm) oxidized the trisradical specials as the crystals were growing slowly over a month, (ii) both trisradical and bisradical crystals formed, but, the crystal of the trisradical could be not distinguishable from the bisradical (in term of morphology), crystals of $C_{82}H_{94}F_{36}N_{16}P_6$ were chosen for crystallography, or (iii) the bisradical state may crystallize preferentially as has been witnessed previously.[5] Although unexpected, this experimental observation is still in keeping with the formation of the trisradical inclusion complex that we observe spectroscopically in solution.

5. ^{1}H NMR Spectroscopy Investigation of Pumping and Dethreading

General procedure for pumping and dethreading experiments: The dumbbell (**DB1**•3PF_6, **DB2**•3PF_6, **DB3**•3PF_6, **DB4**•3PF_6, **DB5**•3PF_6, **DB6**•3PF_6, **DB7**•3PF_6, or **DB8**•3PF_6, 0.001 mmol) and **CBPQT**•4PF_6 (1.1 mg, 0.001 mmol) were dissolved in CD_3CN (0.75 mL, degassed). Excess of Zn dust was added to the solution in a glovebox. The solution changes quickly to a deep blue color and then to purple in seconds. After stirring for 5 min, the mixture is filtered and tris(4-bromophenyl)aminium hexachloridoantimonate (Magic Blue)(5 mg, 0.006 mmol) is added at 0 °C, causing the solution to change color quickly to deep blue. The resulting solution is sealed in an NMR tube and analyzed by ^{1}H NMR spectroscopy.

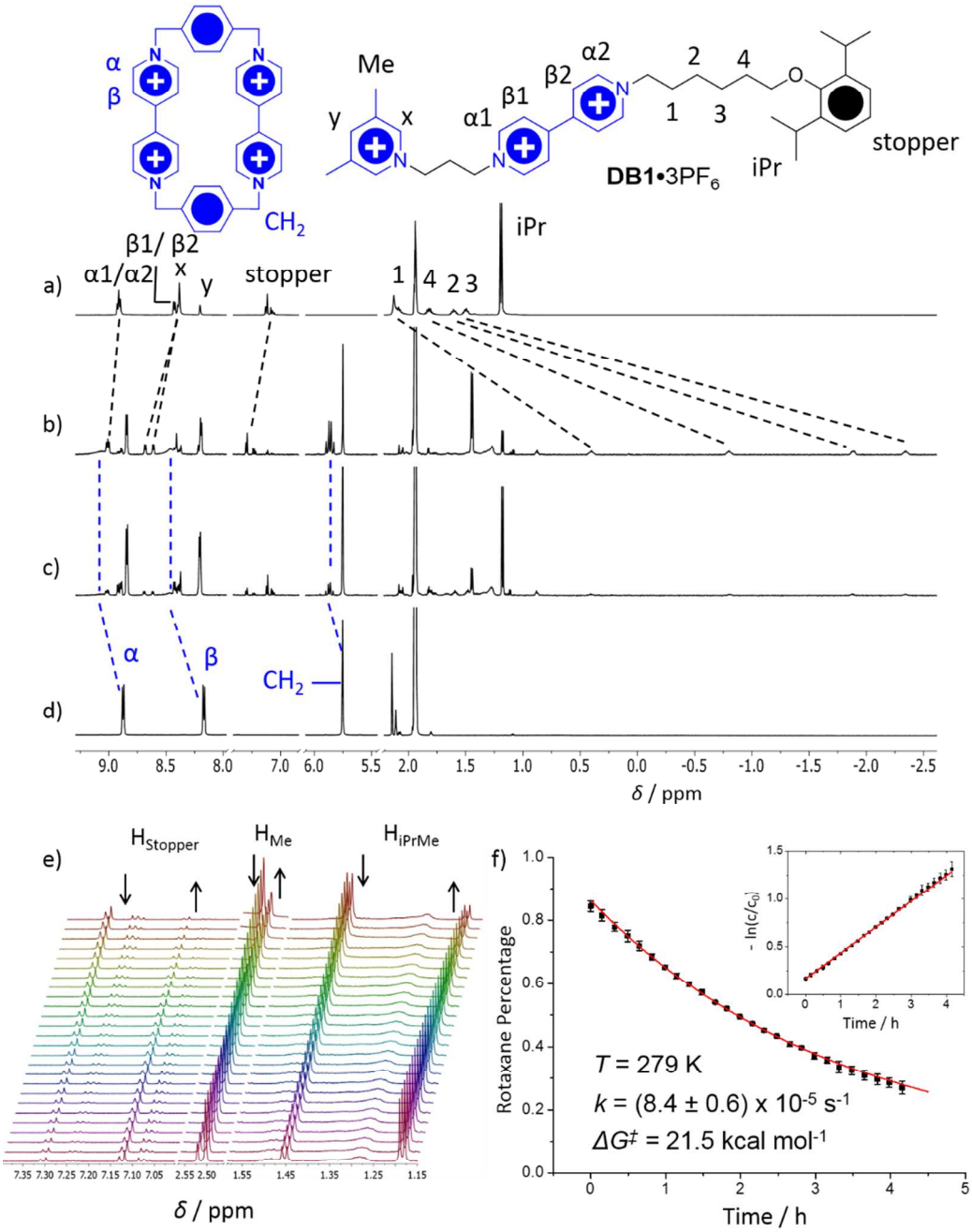

Figure S4. ^{1}H NMR Spectra (recorded in CD_3CN) of a) **DB1**•$3PF_6$, b) **DB1**•$3PF_6$ and **CBPQT**•$4PF_6$ immediately after the reduction and oxidation procedures, and c) after 4 h at 6 °C, and d) **CBPQT**•$4PF_6$. e) ^{1}H NMR Spectra recorded at 6 °C over 4 h. (f) The change in the molar ratio with time based on ^{1}H NMR integration. The inset shows a linear relationship between $-\ln(c/c_0)$ and time, indicating that the dethreading obeys first order kinetics. The activation barrier $\Delta G^{\neq}$ was calculated using the Eyring equation.

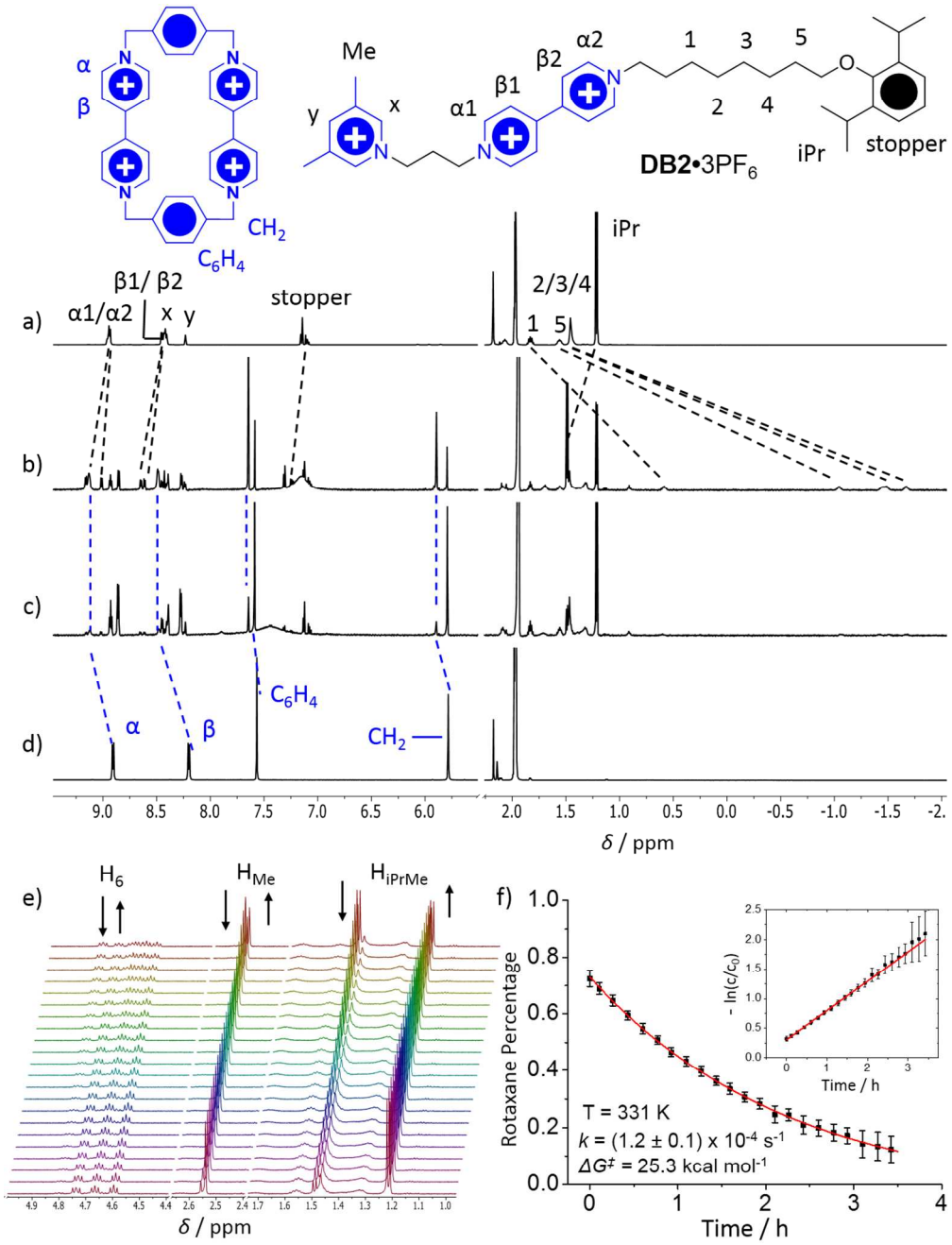

Figure S5. ^{1}H NMR spectra (recorded in CD_3CN) of a) **DB2**•3PF_6, b) **DB2**•3PF_6 and **CBPQT**•4PF_6 immediately after the reduction and oxidation procedures, and c) after 3 h at 58 °C, and d) **CBPQT**•4PF_6. e) ^{1}H NMR Spectra recorded at 58 °C over 3 h. (f) The change in the molar ratio with time based on ^{1}H NMR integration. The inset shows a linear relationship between $-\ln(c/c_0)$ and time, indicating that the dethreading obeys first order kinetics. The activation barrier $\Delta G^{\neq}$ was calculated using the Eyring equation.

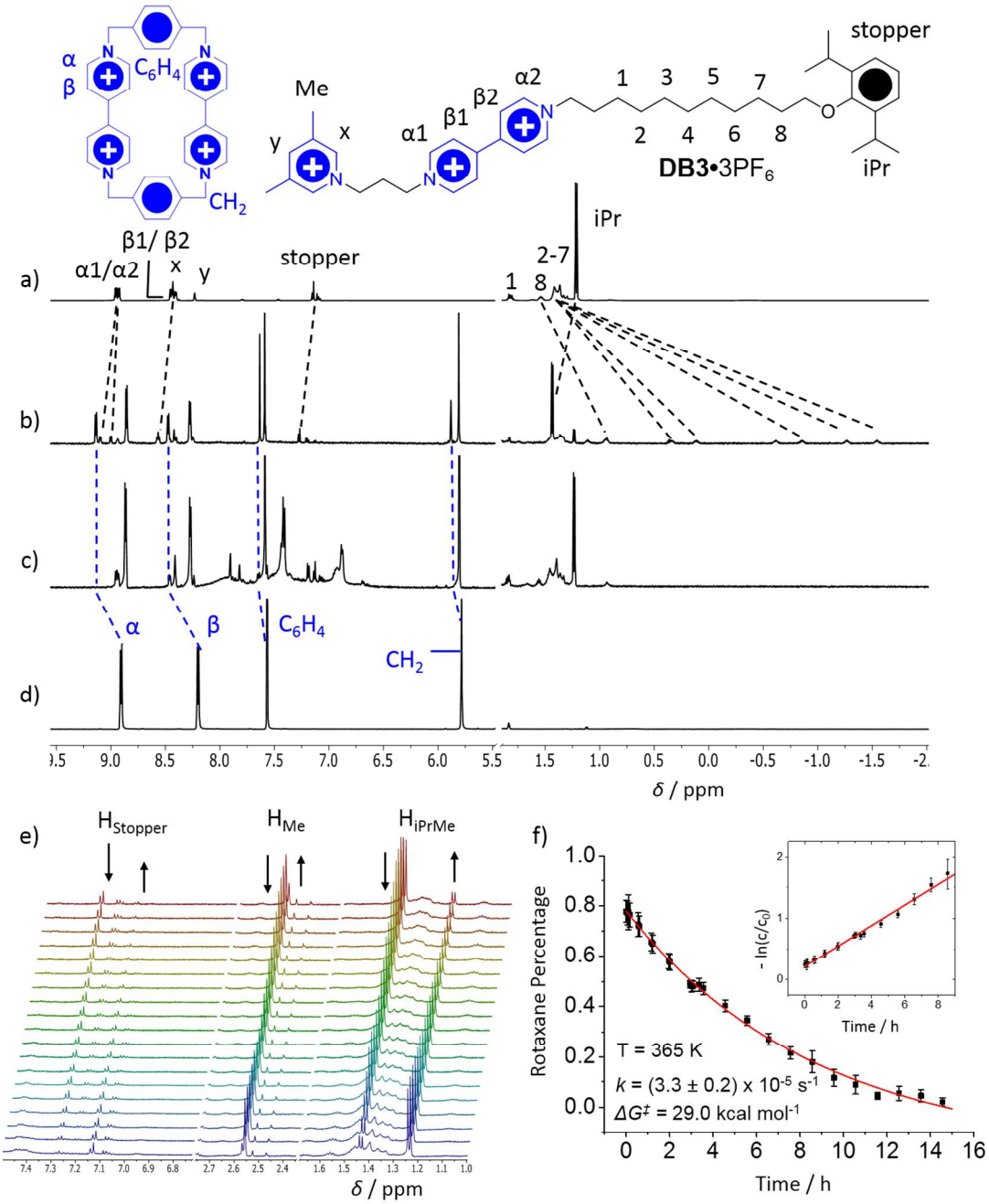

Figure S6. ^{1}H NMR Spectra (recorded in CD_3CN) of a) **DB3**•3PF_6, b) **DB3**•3PF_6 and **CBPQT**•4PF_6 immediately after the reduction and oxidation procedures, and c) after 14 h at 92 °C, and d) **CBPQT**•4PF_6. e) ^{1}H NMR Spectra recorded at 92 °C over 14 h. (f) The change in the molar ratio with time based on ^{1}H NMR integration. The inset shows a linear relationship between $-\ln(c/c_0)$ and time, indicating that the dethreading obeys first order kinetics. The activation barrier $\Delta G^{\neq}$ was calculated using the Eyring equation.

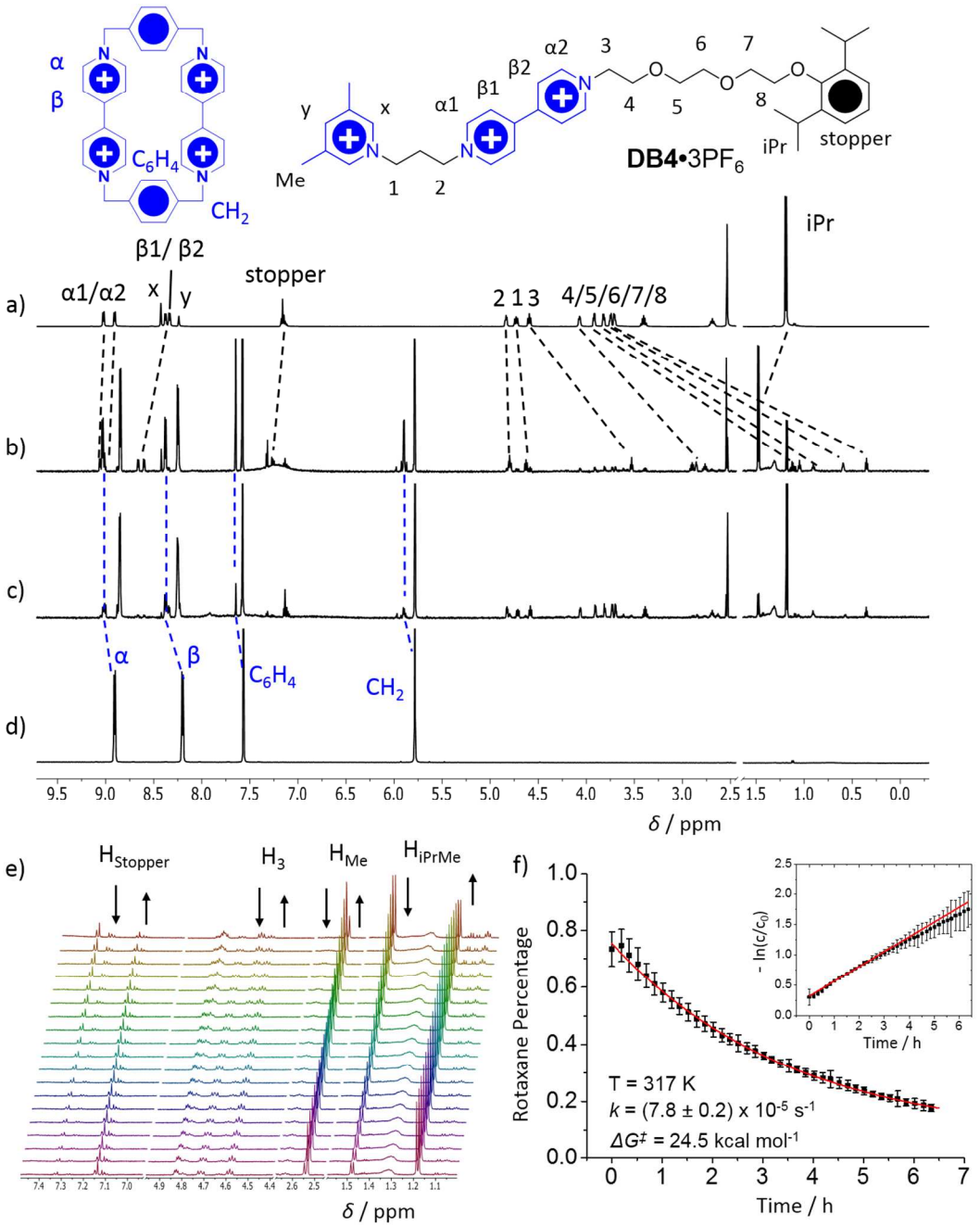

Figure S7. ^{1}H NMR Spectra (recorded in CD_3CN) of a) **DB4**•$3PF_6$, b) **DB4**•$3PF_6$ and **CBPQT**•$4PF_6$ immediately after the reduction and oxidation procedures, and c) after 6 h at 44 °C, and d) **CBPQT**•$4PF_6$. e) ^{1}H NMR Spectra recorded at 44 °C over 6 h. (f) The change in the molar ratio with time based on ^{1}H NMR integration. The inset shows a linear relationship between $-\ln(c/c_0)$ and time, indicating that the dethreading obeys first order kinetics. The activation barrier $\Delta G^{\neq}$ was calculated using the Eyring equation.

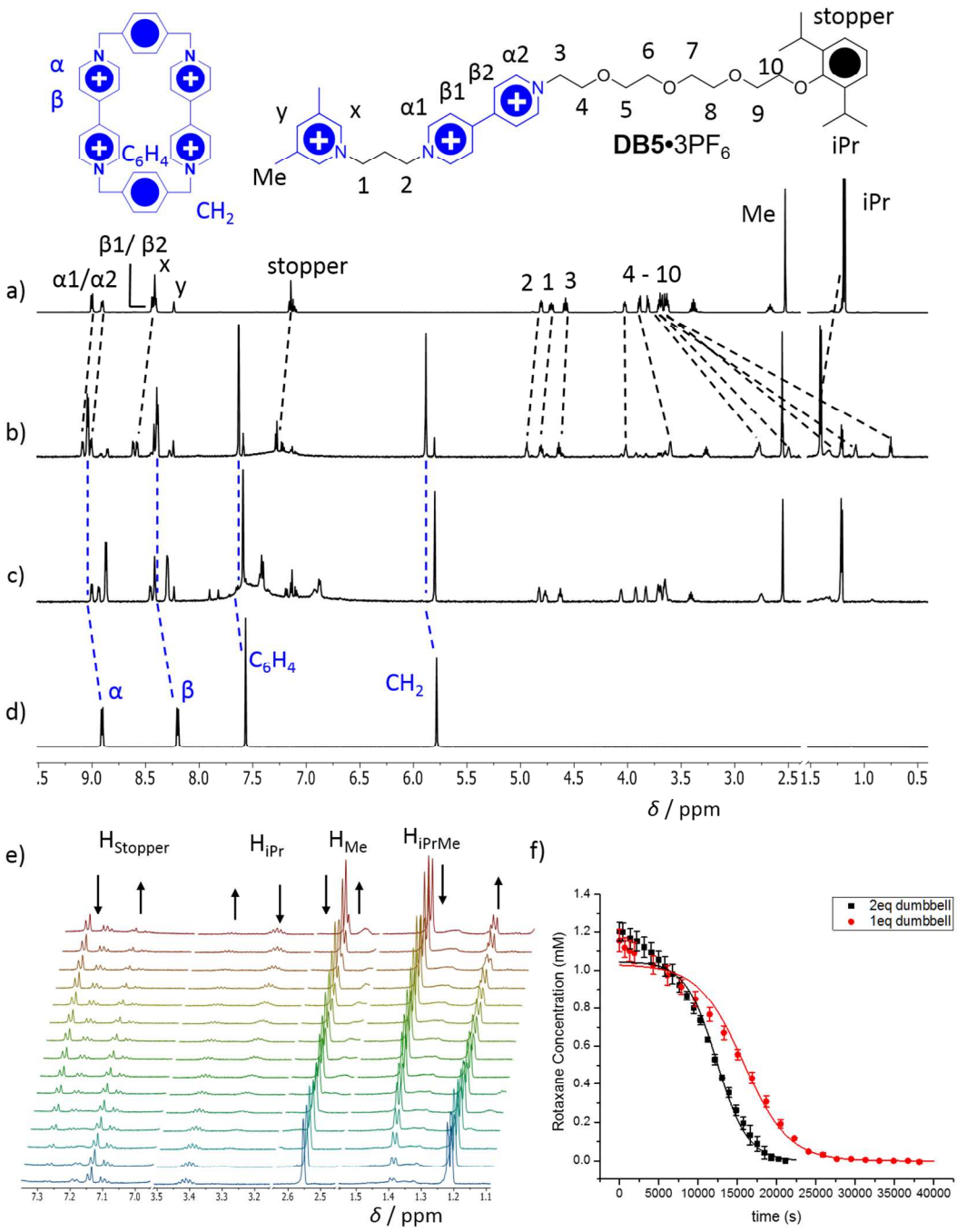

Figure S8. ^{1}H NMR spectra (recorded in CD_3CN) of a) **DB5**•$3PF_6$, b) **DB5**•$3PF_6$ and **CBPQT**•$4PF_6$ immediately after the reduction and oxidation procedures, and c) after 10 h at 82 °C, and d) **CBPQT**•$4PF_6$. e) ^{1}H NMR Spectra recorded at 82 °C over 10 h. (f) The change in the molar ratio with time based on ^{1}H NMR integration; the S shape curve indicating the dethreading is indicative of an auto-catalytic process.

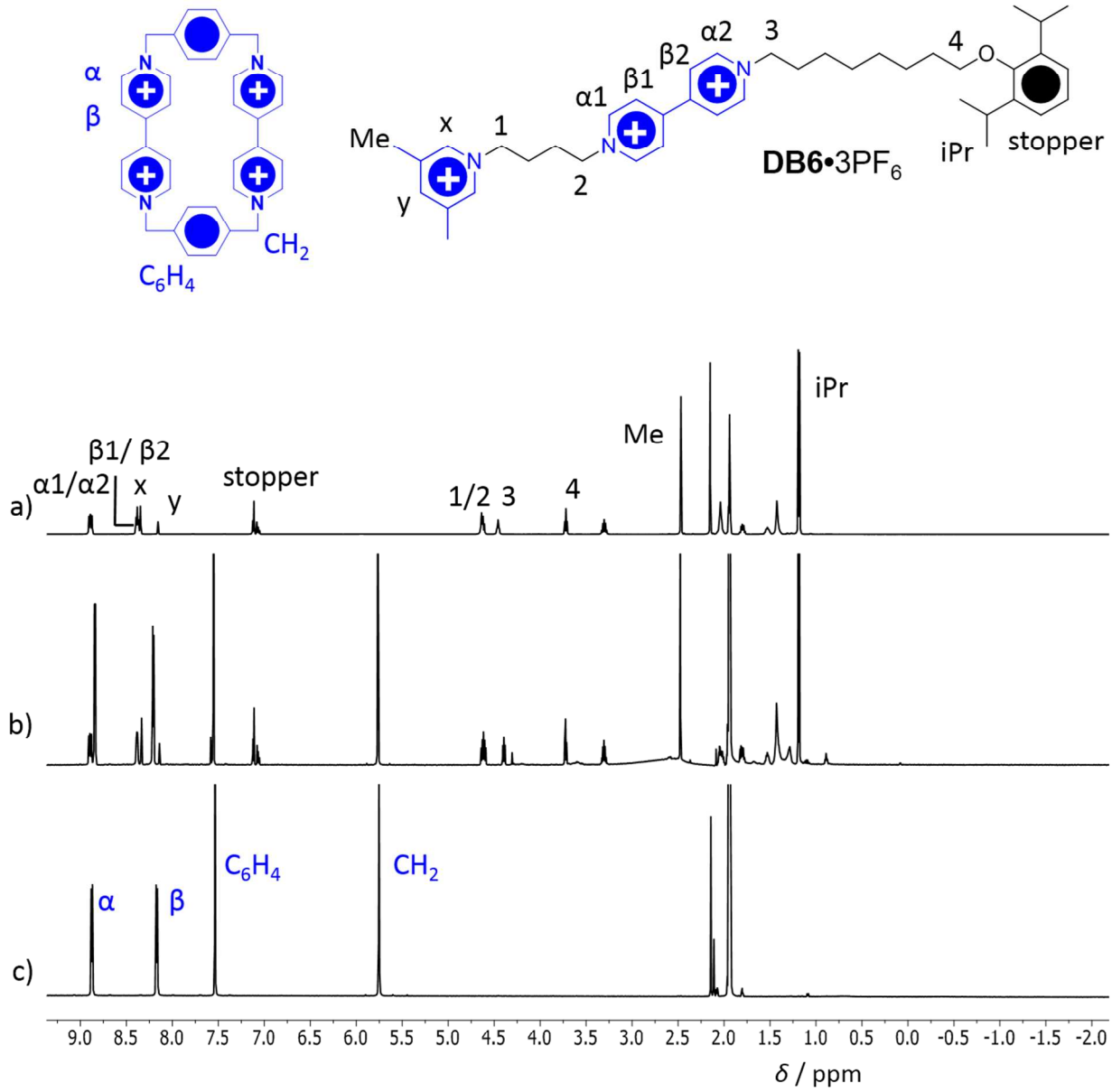

Figure S9. ^{1}H NMR Spectra (CD_3CN, 298 K) of a) **DB6**•3PF_6, b) **DB6**•3PF_6 and **CBPQT**•4PF_6 immediately after the reduction and oxidation procedures, and c) **CBPQT**•4PF_6. No obvious shifts were identified indicating that the spectrum b) is a simple physical mixture of **DB6**•3PF_6 and **CBPQT**•4PF_6

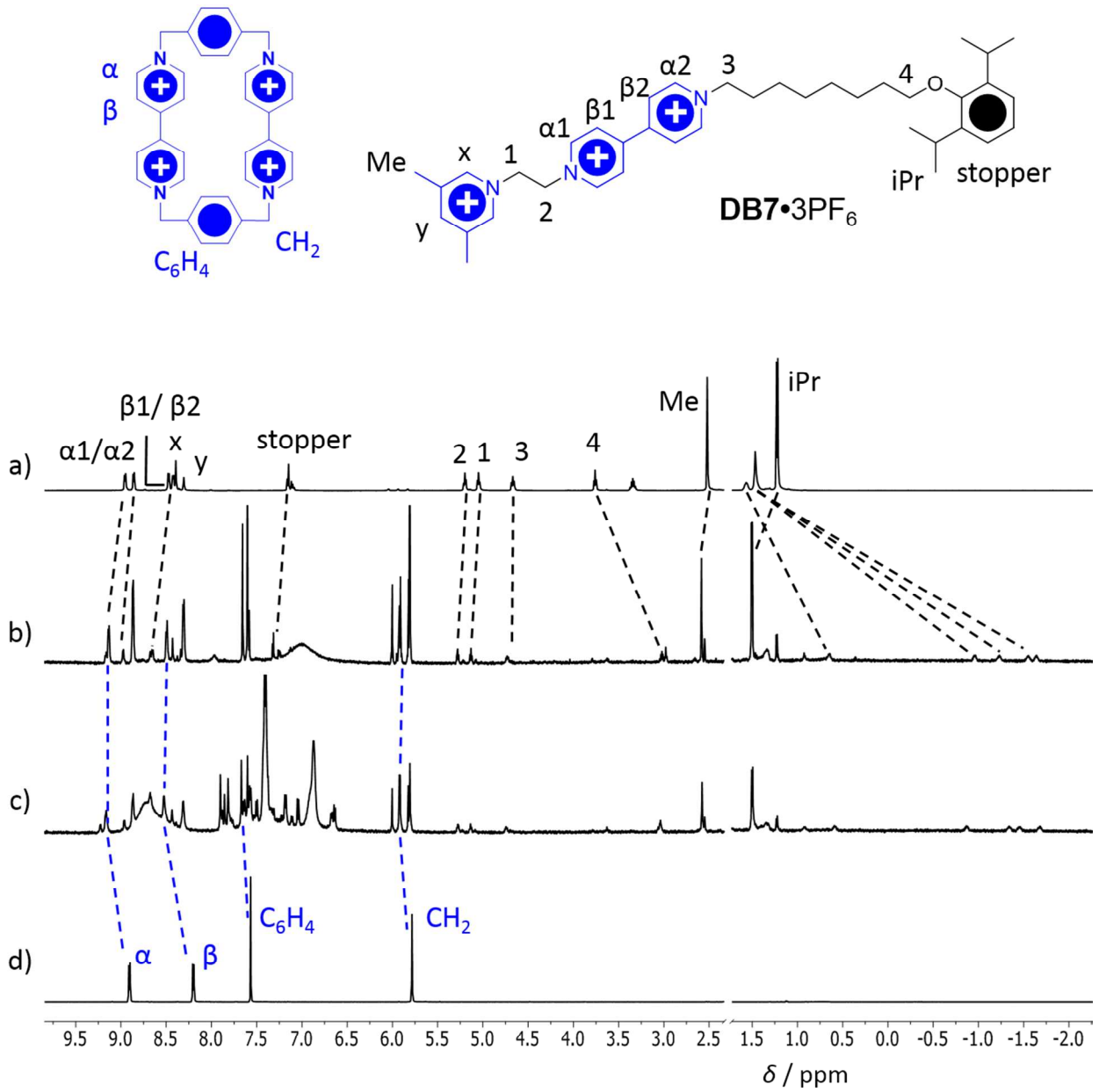

Figure S10. ^{1}H NMR Spectra (recorded in CD_3CN) of a) **DB7**•3PF_6, b) **DB7**•3PF_6 and **CBPQT**•4PF_6 immediately after the reduction and oxidation procedures, and c) after 18 h at 82 °C, and d) **CBPQT**•4PF_6. The spectrum of the mixture of **DB7**•3PF_6 and **CBPQT**•4PF_6 after the reduction and oxidation procedure does not change at high temperature over several hours (cf. b and c) indicating the dethreading barrier for **CBPQT**$^{4+}$ is high. Additional peaks in aromatic area are attributed to the decomposition of Magic Blue upon subjecting to high temperature over an extended period of time.

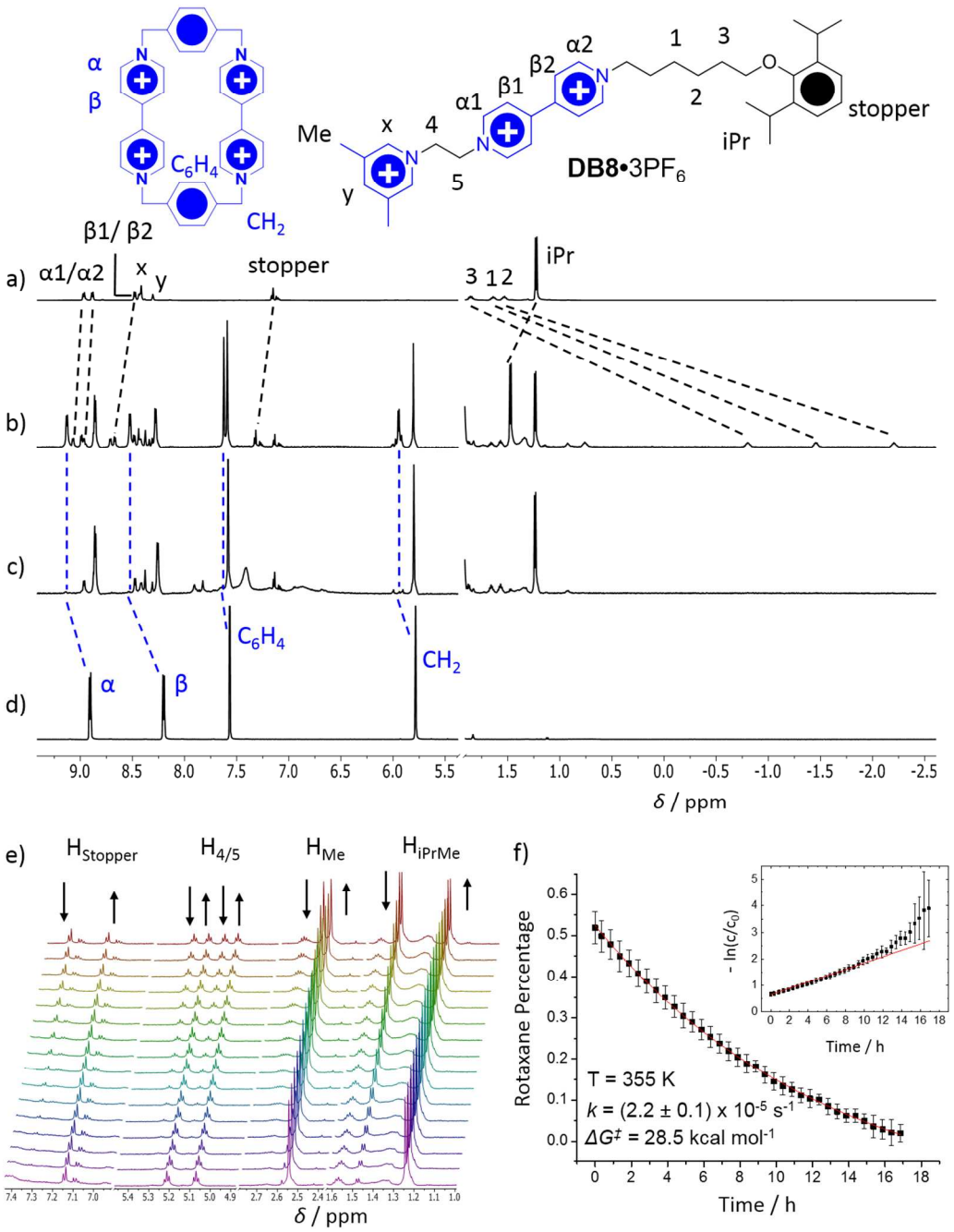

Figure S11. ^{1}H NMR Spectra (recorded in CD_3CN) of a) **DB8**•3PF_6, b) **DB8**•3PF_6 and **CBPQT**•4PF_6 immediately after the reduction and oxidation procedures, and c) after 16 h at 82 °C, d) **CBPQT**•4PF_6. e) ^{1}H NMR Spectra recorded at 82 °C over 16 h. (f) The change in the molar ratio with time based on ^{1}H NMR integration. The inset shows a linear relationship between $-\ln(c/c_0)$ and time, indicating that the dethreading obeys first order kinetics. The activation barrier $\Delta G^{\neq}$ was calculated using the Eyring equation.

Table S1. **Summary of Thermodynamic Data.**

Compound	Dethreading rate constant k / 10^{-5} s^{-1} (Temperature / K)	Activation barrier [a] $\Delta G^{\neq}$ / kcal mol^{-1}	Half life time [b] $t_{1/2}$ at 298 K / h
DB1•3PF_6	8.4 ± 0.6 (279)	21.5	0.18
DB2•3PF_6	12 ± 1 (331)	25.3	120
DB3•3PF_6	3.3 ± 0.2 (365)	29.0	57000
DB4•3PF_6	7.8 ± 0.2 (317)	24.5	32
DB5•3PF_6	-	-	-
DB6•3PF_6	> 1000 (298)	< 18.3	< 0.01
DB7•3PF_6	< 0.05 (355)	> 31.3	> 2900000
DB8•3PF_6	2.2 ± 0.1 (355)	28.5	24000

[a] Calculated using the Erying equation using the detheading rate constant. [b] Calculated using $t_{1/2}$ = ln2 / k_{298K}, where k_{298K} is the dethreading rate constant at 298 K where can be obtained using the Eyring equation with $\Delta G^{\ddagger}$, assuming the temperature dependence of $\Delta G^{\ddagger}$ can be ignored.

Table S2. Summary of Rotaxane Yield at Different Oxidization Temperatures.[a]

Dumbbell	Yield (%)		
	RT	0°C	–40°C
DB7•3PF_6	79	83	-
DB2•3PF_6	50	74	>95
DB6•3PF_6	0	0	<5

[a] Dumbell (1.0 mg, 0.001 mmol) and **CBPQT**•4PF_6 (1.1 mg, 0.001 mmol) was dissolved in CD_3CN (0.75 mL, degassed). Excess of Zn dust was added to the solution in a glovebox. After stirring for 5 min, the mixture was filtered and tris(4-bromophenyl)aminium hexachloridoantimonate (Magic Blue, 5 mg, 0.006 mmol) was added at the given temperature before the sample was analyzed by ^{1}H NMR at that temperature.

6. DFT calculations

The geometries were optimized using the PBF Poisson-Boltzmann solvation model[6] for acetonitrile (ε=37.5 and R_0= 2.18 Å) at the level of M06-HF/6-31G* with Jaguar 7.9[7]. The single point energy was refined at the level of M06-HF/6-311++G**. We assumed that two MeCN molecules are contained in the cavity of free **CBPQT**$^{4+}$ in solution. The energies of **DB1**$^{3+}$, **DB2**$^{3+}$, **DB3**$^{3+}$ and corresponding **CBPQT**$^{4+}$ rotaxanes are listed in **Table S3**.

In order to obtain the potential profile for the dethreading process for **DB8**$^{3+}$ and **DB9**$^{3+}$, the center of the **CBPQT**$^{4+}$ ring was scanned along each atom of the molecule. Various numbers of chloride anions (0–3) were placed around the molecule as counterions to accommodate better the change of electrostatics as a result of the motion of **CBPQT**$^{4+}$ ring. Then the minimum energy was evaluated for each point along the potential profile. The barrier was calculated as the energy difference between the highest point in the potential profile and the rotaxane with **CBPQT**$^{4+}$ optimized with no constraint at the end of diisopropylphenol (defined as freely optimized in the **Table S4** and **S11**).

The total energy is the sum of refined single point energy and solvation energy, as provided in the **Table S4−13**. The gas phase energy is the DFT energy for a vacuum with no corrections for zero-point energy (ZPE). The solution phase energy includes the solute energy and half of the solute-solvent energy. The solvation energy is the difference between these two quantities. The refined single point energy is the DFT energy for a vacuum at 6-311++G** level. The difference between refined single point energy in column 5 and gas phase energy in column 3 is subtracted from solution phase energy in column 2 to give the total energy in column 6. This total energy does not include the effects of entropy and specific heat needed to get the free energy at the

temperature of the experiments. The total energy is the quantity to be used in considering the energy profiles.

Table S3. The energy components of **DB1**$^{3+}$, **DB2**$^{3+}$, **DB3**$^{3+}$, **CBPQT**$^{4+}$ and corresponding [2]pseudorotaxanes.

	solution phase energy	**gas phase energy**	**solvation energy**	**refined single point energy**	**total energy**
DB1^{3+}	-1717.915627	-1717.46068	-0.454946	-1717.918433	-1718.37338
DB2^{3+}	-1796.513915	-1796.060229	-0.453685	-1796.538531	-1796.99222
DB3^{3+}	-1914.410262	-1913.958397	-0.451865	-1914.467299	-1914.91916
DB1^{3+}⊂**CBPQT**$^{4+}$	-3326.993458	-3325.360269	-1.633189	-3326.241829	-3327.87502
DB2^{3+}⊂**CBPQT**$^{4+}$	-3405.602955	-3404.03155	-1.571406	-3404.932268	-3406.50367
DB3^{3+}⊂**CBPQT**$^{4+}$	-3523.502404	-3522.009906	-1.492498	-3522.940921	-3524.43342
CBPQT^{4+}	-1609.101228	-1608.353963	-0.747265	-1608.770372	-1609.51764
2CH_3CN⊂**CBPQT**$^{4+}$	-1874.547038	-1873.80792	-0.739117	-1874.311107	-1875.05022
CH_3CN	-265.4362174	-265.4159063	-0.020311	-265.5044871	-265.524798

Table S4. The energy components of **CBPQT**$^{4+}$ moving on **DB8**$^{3+}$ with no Cl^-.

	solution phase energy	gas phase energy	solvation energy	refined single point energy	total energy
DB8^{3+}	-1678.605646	-1678.138209	-0.467437573	-1678.585992	-1679.05343
Freely optimized	-3287.684173	-3286.035138	-1.649035	-3286.906831	-3288.555865
C1	-3287.640671	-3285.910133	-1.730538	-3286.786004	-3288.516543
C2	-3287.632835	-3285.841534	-1.791301	-3286.719131	-3288.510432
C3	-3287.631109	-3285.820389	-1.810720	-3286.698749	-3288.509470
N4	-3287.631680	-3285.773063	-1.858617	-3286.657305	-3288.515922
C5	-3287.628561	-3285.761729	-1.866832	-3286.639066	-3288.505898
C6	-3287.619369	-3285.752630	-1.866739	-3286.630015	-3288.496754
C7	-3287.616599	-3285.754825	-1.861774	-3286.633371	-3288.495145
C8	-3287.611596	-3285.747270	-1.864326	-3286.627459	-3288.491785
C9	-3287.594925	-3285.740370	-1.854555	-3286.618297	-3288.472852
C10	-3287.585364	-3285.741071	-1.844293	-3286.619557	-3288.463850
N11	-3287.588307	-3285.743732	-1.844575	-3286.622722	-3288.467297
C12	-3287.587636	-3285.740688	-1.846949	-3286.621582	-3288.468530
C13	-3287.602383	-3285.754552	-1.847831	-3286.636082	-3288.483913

N14	-3287.617305	-3285.773445	-1.843860	-3286.653574	-3288.497434
C15	-3287.614383	-3285.770039	-1.844345	-3286.651124	-3288.495468
C16	-3287.615633	-3285.780277	-1.835355	-3286.660149	-3288.495505

Table S5. The energy components of **CBPQT**$^{4+}$ moving on **DB8**$^{3+}$ with 1 Cl^- (configuration 1)

	solution phase energy	**gas phase energy**	**solvation energy**	**refined single point energy**	**total energy**
Cl^-	-460.3496276	-460.2279551	-0.121672512	-460.2818989	-460.418929
C1	-3748.006557	-3746.714496	-1.292060	-3747.653265	-3748.945326
C2	-3747.999340	-3746.655132	-1.344208	-3747.595416	-3748.939624
C3	-3747.999884	-3746.640569	-1.359315	-3747.582142	-3748.941457
N4	-3747.997610	-3746.598779	-1.398832	-3747.541566	-3748.940398
C5	-3748.003824	-3746.587069	-1.416756	-3747.530304	-3748.947059
C6	-3747.992931	-3746.565397	-1.427535	-3747.509898	-3748.937433
C7	-3747.987460	-3746.548395	-1.439065	-3747.499327	-3748.938392
C8	-3747.978545	-3746.538456	-1.440089	-3747.491297	-3748.931387
C9	-3747.981306	-3746.545953	-1.435353	-3747.488362	-3748.923715
C10	-3747.988904	-3746.566784	-1.422120	-3747.508555	-3748.930675
N11	-3747.980235	-3746.564116	-1.416119	-3747.506165	-3748.922284
C12	-3748.008053	-3746.570663	-1.437389	-3747.513719	-3748.951109
C13	-3747.992984	-3746.576974	-1.416011	-3747.521433	-3748.937444

N14	-3748.007000	-3746.594845	-1.412154	-3747.537920	-3748.950074
C15	-3748.012157	-3746.599785	-1.412372	-3747.542888	-3748.955260
C16	-3748.002847	-3746.597855	-1.404993	-3747.539502	-3748.944495

Table S6. The energy components of **CBPQT**$^{4+}$ moving on **DB8**$^{3+}$ with 1 Cl^-.(configuration 2)

	solution phase energy	**gas phase energy**	**solvation energy**	**refined single point energy**	**total energy**
C1	-3747.954454	-3746.633637	-1.320816	-3747.573719	-3748.894535
C2	-3747.984457	-3746.620162	-1.379178	-3747.564755	-3748.943933
C3	-3747.990155	-3746.608414	-1.391470	-3747.553749	-3748.945219
N4	-3747.986162	-3746.594866	-1.402745	-3747.538944	-3748.941688
C5	-3747.986090	-3746.579688	-1.424136	-3747.523829	-3748.947966
C6	-3747.986334	-3746.560331	-1.432601	-3747.506884	-3748.939484
C7	-3747.983956	-3746.559461	-1.427999	-3747.503215	-3748.931214
C8	-3747.975012	-3746.552480	-1.426065	-3747.498051	-3748.924116
C9	-3747.951588	-3746.541770	-1.439536	-3747.486551	-3748.926087
C10	-3747.962989	-3746.544227	-1.444677	-3747.487310	-3748.931988
N11	-3747.965594	-3746.545618	-1.434616	-3747.488386	-3748.923002
C12	-3747.970630	-3746.568313	-1.439740	-3747.512162	-3748.951901

C13	-3747.984963	-3746.566439	-1.426545	-3747.520090	-3748.946635
N14	-3747.997611	-3746.586135	-1.420864	-3747.532033	-3748.952897
C15	-3748.001689	-3746.591399	-1.420758	-3747.534899	-3748.955657
C16	-3748.009065	-3746.597792	-1.405056	-3747.540877	-3748.945933

Table S7. The energy components of **CBPQT**$^{4+}$ moving on **DB8**$^{3+}$ with 2 Cl^-(configuration 1)

	solution phase energy	**gas phase energy**	**solvation energy**	**refined single point energy**	**total energy**
C1	-4208.344577	-4207.378152	-0.966425	-4208.379425	-4209.345850
C2	-4208.358055	-4207.359675	-0.998380	-4208.360738	-4209.359118
C3	-4208.353949	-4207.351684	-1.002265	-4208.353820	-4209.356085
N4	-4208.359548	-4207.328584	-1.030964	-4208.333492	-4209.364456
C5	-4208.352082	-4207.328762	-1.023319	-4208.335019	-4209.358338
C6	-4208.351969	-4207.315437	-1.036532	-4208.323229	-4209.359761
C7	-4208.349021	-4207.307683	-1.041338	-4208.314871	-4209.356209
C8	-4208.344373	-4207.299377	-1.044995	-4208.306394	-4209.351389
C9	-4208.344988	-4207.304264	-1.040724	-4208.311100	-4209.351824
C10	-4208.358575	-4207.325293	-1.033283	-4208.331964	-4209.365247
N11	-4208.362071	-4207.326534	-1.035537	-4208.332417	-4209.367954
C12	-4208.352463	-4207.331863	-1.020600	-4208.338604	-4209.359203

C13	-4208.363247	-4207.339074	-1.024173	-4208.344680	-4209.368854
N14	-4208.379051	-4207.346382	-1.032669	-4208.351221	-4209.383890
C15	-4208.379146	-4207.348612	-1.030534	-4208.353274	-4209.383809
C16	-4208.381736	-4207.373363	-1.008374	-4208.376534	-4209.384908

Table S8. The energy components of **CBPQT**$^{4+}$ moving on **DB8**$^{3+}$ with 2 Cl^-(configuration 2)

	solution phase energy	**gas phase energy**	**solvation energy**	**refined single point energy**	**total energy**
C1	-4208.344932	-4207.403938	-0.940994	-4208.405109	-4209.346103
C2	-4208.351621	-4207.390258	-0.961363	-4208.393501	-4209.354863
C3	-4208.361373	-4207.377600	-0.983773	-4208.380335	-4209.364108
N4	-4208.372490	-4207.360509	-1.011981	-4208.365245	-4209.377226
C5	-4208.369254	-4207.342461	-1.026793	-4208.347906	-4209.374699
C6	-4208.351805	-4207.318367	-1.033438	-4208.324691	-4209.358129
C7	-4208.342178	-4207.313528	-1.028649	-4208.321986	-4209.350635
C8	-4208.349002	-4207.306222	-1.042780	-4208.313462	-4209.356241
C9	-4208.353965	-4207.304617	-1.049348	-4208.312405	-4209.361753
C10	-4208.352116	-4207.311727	-1.040389	-4208.318346	-4209.358735
N11	-4208.352689	-4207.314216	-1.038473	-4208.320762	-4209.359235
C12	-4208.356528	-4207.333037	-1.023491	-4208.340115	-4209.363605

C13	-4208.359308	-4207.339431	-1.019876	-4208.344686	-4209.364562
N14	-4208.374895	-4207.343072	-1.031823	-4208.347765	-4209.379589
C15	-4208.378811	-4207.348003	-1.030808	-4208.352280	-4209.383088
C16	-4208.374978	-4207.365051	-1.009928	-4208.367407	-4209.377335

Table S9. The energy components of **CBPQT**$^{4+}$ moving on **DB8**$^{3+}$ with 3 Cl^-(configuration 1)

	solution phase energy	**gas phase energy**	**solvation energy**	**refined single point energy**	**total energy**
C1	-4668.670563	-4667.926512	-0.744051	-4668.987758	-4669.731808
C2	-4668.692034	-4667.948030	-0.744004	-4669.010870	-4669.754874
C3	-4668.696411	-4667.966856	-0.729555	-4669.032729	-4669.762284
N4	-4668.708114	-4667.972124	-0.735990	-4669.039579	-4669.775570
C5	-4668.704431	-4667.960150	-0.744281	-4669.028412	-4669.772692
C6	-4668.703570	-4667.957238	-0.746332	-4669.026824	-4669.773156
C7	-4668.699852	-4667.953018	-0.746834	-4669.022905	-4669.769739
C8	-4668.703950	-4667.955866	-0.748084	-4669.025223	-4669.773307
C9	-4668.702406	-4667.970373	-0.732034	-4669.038614	-4669.770648
C10	-4668.717918	-4667.989332	-0.728586	-4669.058116	-4669.786702
N11	-4668.711727	-4667.987387	-0.724340	-4669.055259	-4669.779599
C12	-4668.707990	-4667.987683	-0.720307	-4669.057581	-4669.777888

C13	-4668.700961	-4667.982158	-0.718803	-4669.052960	-4669.771763
N14	-4668.695862	-4667.981650	-0.714212	-4669.050278	-4669.764489
C15	-4668.710142	-4668.000267	-0.709875	-4669.067671	-4669.777546
C16	-4668.738442	-4668.031843	-0.706599	-4669.096541	-4669.803140

Table S10. The energy components of **CBPQT**$^{4+}$ moving on **DB8**$^{3+}$ with 3 Cl^-(configuration 2)

	solution phase energy	**gas phase energy**	**solvation energy**	**refined single point energy**	**total energy**
C1	-4668.694627	-4668.031238	-0.663390	-4669.096383	-4669.759773
C2	-4668.705877	-4668.031723	-0.674155	-4669.094609	-4669.768764
C3	-4668.714858	-4668.033028	-0.681830	-4669.096524	-4669.778354
N4	-4668.728000	-4668.026350	-0.701650	-4669.090137	-4669.791787
C5	-4668.736651	-4668.020157	-0.716495	-4669.085408	-4669.801903
C6	-4668.724337	-4668.006362	-0.717976	-4669.070693	-4669.788669
C7	-4668.723167	-4668.007802	-0.715366	-4669.073514	-4669.788880
C8	-4668.725131	-4668.005714	-0.719417	-4669.073466	-4669.792883
C9	-4668.733565	-4668.016388	-0.717177	-4669.085789	-4669.802966
C10	-4668.713336	-4668.000111	-0.713225	-4669.066846	-4669.780071
N11	-4668.710112	-4667.995360	-0.714752	-4669.061923	-4669.776676
C12	-4668.708123	-4667.986329	-0.721794	-4669.056142	-4669.777936

C13	-4668.703208	-4667.986234	-0.716974	-4669.057039	-4669.774013
N14	-4668.699105	-4667.992169	-0.706936	-4669.060309	-4669.767244
C15	-4668.722671	-4668.000410	-0.722262	-4669.065067	-4669.787329
C16	-4668.728823	-4668.019349	-0.709474	-4669.083801	-4669.793275

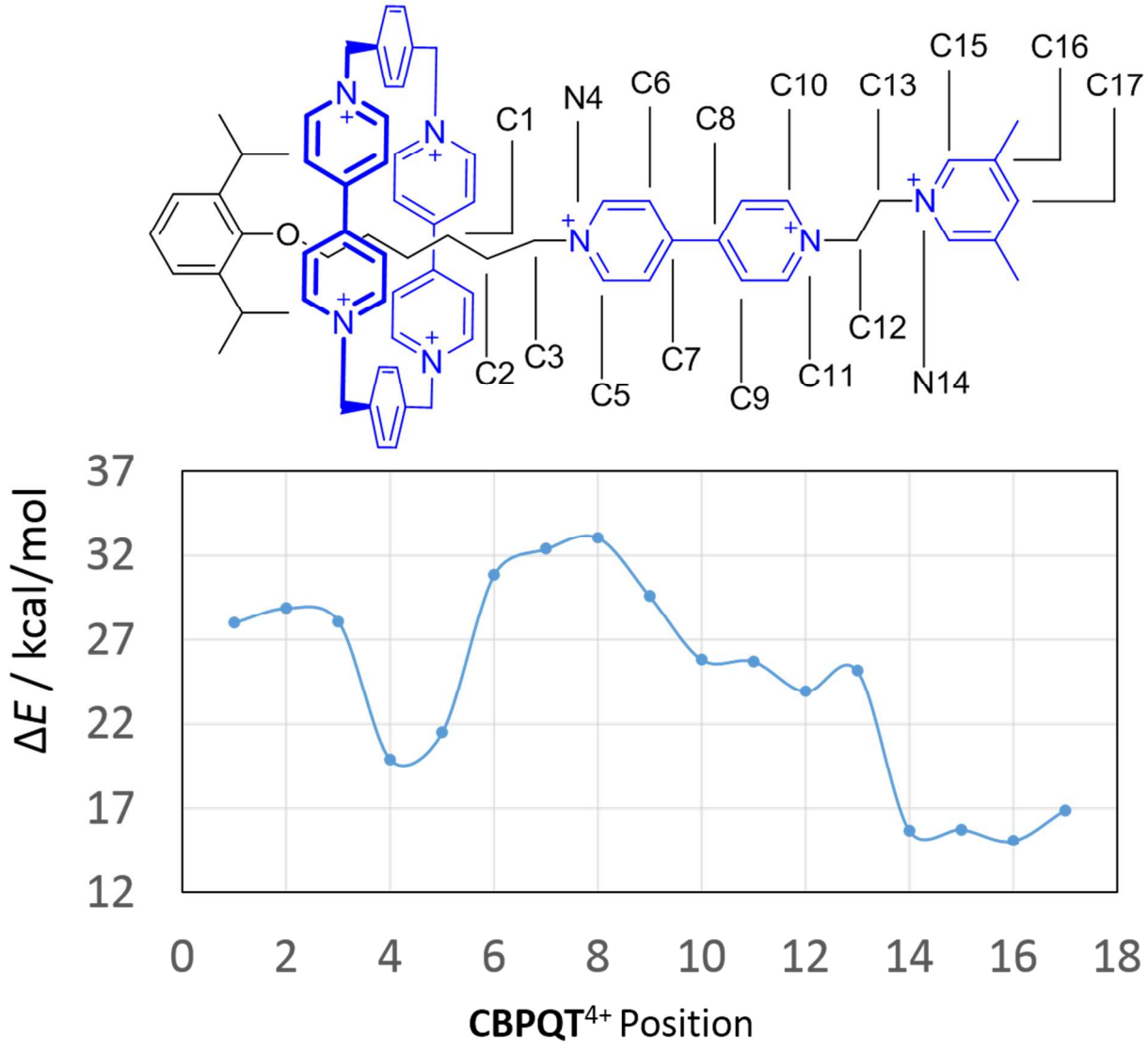

Figure S12. The potential energy surface of **CBPQT**$^{4+}$ moving on **DB8**$^{3+}$. These energies are enthalpies at 0K, except that we do not include zero point energy (the solvation correction is a free energy at 300K). The reference is at infinite separation. The energy of

the rotaxane with **CBPQT**$^{4+}$ optimized with no constraint at the end of diisopropylphenol is 14.4 kcal/mol, leading to the dethreading enthalpic barrier 18.7 kcal/mol. This can be compared to experimental dethreading free energy barrier of 28.5 kcal mol^{-1} for **DB8**$^{3+}$⊂**CBPQT**$^{4+}$. The discrepancy probably arises because the theory does not include ZPE or entropic affects.

Table S11. The energy components of **CBPQT**$^{4+}$ moving on **DB9**$^{3+}$ with no Cl^-

	solution phase energy	gas phase energy	solvation energy	refined single point energy	total energy
DB9^{3+}	-1757.202934	-1756.737549	-0.465385446	-1757.205813	-1757.671200
freely optimized	-3366.297002	-3364.692622	-1.604379	-3365.583946	-3367.188326
C1	-3366.256609	-3364.569436	-1.687172	-3365.464766	-3367.151939
C2	-3366.248275	-3364.506685	-1.741590	-3365.293463	-3367.035052
C3	-3366.246115	-3364.486493	-1.759622	-3365.385346	-3367.144968
N4	-3366.247019	-3364.447489	-1.799530	-3365.347336	-3367.146866
C5	-3366.245675	-3364.431896	-1.813779	-3365.324066	-3367.137845
C6	-3366.244950	-3364.421083	-1.823866	-3365.319231	-3367.143097
C7	-3366.251536	-3364.404100	-1.847436	-3365.303069	-3367.150505
C8	-3366.233153	-3364.406531	-1.826622	-3365.305730	-3367.132351
C9	-3366.236909	-3364.406010	-1.830899	-3365.303678	-3367.134578
C10	-3366.231492	-3364.407074	-1.824419	-3365.304049	-3367.128467
N11	-3366.223617	-3364.407401	-1.816216	-3365.304864	-3367.121080
C12	-3366.219384	-3364.405907	-1.813477	-3365.303340	-3367.116817
C13	-3366.208671	-3364.401564	-1.807107	-3365.299409	-3367.106515
C14	-3366.217241	-3364.420046	-1.797196	-3365.316810	-3367.114005
C15	-3366.240196	-3364.439487	-1.800710	-3365.337140	-3367.137850
N16	-3366.253825	-3364.467439	-1.786386	-3365.362689	-3367.149074
C17	-3366.254024	-3364.474362	-1.779662	-3365.371612	-3367.151274
C18	-3366.259237	-3364.491081	-1.768156	-3365.385847	-3367.154003
C19	-3366.275421	-3364.518585	-1.756836	-3365.412665	-3367.169501

Table S12. The energy components of **CBPQT**$^{4+}$ moving on **DB9**$^{3+}$ with 1 Cl^-(configuration 1)

	solution phase energy	gas phase energy	solvation energy	refined single point energy	total energy
C1	-3826.614312	-3825.360641	-1.253671	-3826.319661	-3827.573331
C2	-3826.603324	-3825.305957	-1.297367	-3826.265339	-3827.562706
C3	-3826.601705	-3825.271602	-1.330104	-3826.235048	-3827.565151
N4	-3826.602025	-3825.251300	-1.350725	-3826.215420	-3827.566145
C5	-3826.604911	-3825.244244	-1.360667	-3826.208640	-3827.569307
C6	-3826.606000	-3825.225201	-1.380799	-3826.190727	-3827.571526
C7	-3826.609218	-3825.215229	-1.393989	-3826.181742	-3827.575731
C8	-3826.613981	-3825.205766	-1.408215	-3826.178899	-3827.587114
C9	-3826.602980	-3825.198250	-1.404731	-3826.167722	-3827.572452
C10	-3826.598444	-3825.200552	-1.397892	-3826.164879	-3827.562771
N11	-3826.595411	-3825.199625	-1.395785	-3826.164986	-3827.560771
C12	-3826.593172	-3825.210754	-1.382418	-3826.182247	-3827.564665
C13	-3826.587090	-3825.206898	-1.380192	-3826.169078	-3827.549270
C14	-3826.606684	-3825.241169	-1.365515	-3826.201287	-3827.566802
C15	-3826.614165	-3825.251912	-1.362253	-3826.211863	-3827.574116
N16	-3826.639110	-3825.276204	-1.362907	-3826.239320	-3827.602226
C17	-3826.642040	-3825.279608	-1.362432	-3826.242846	-3827.605279
C18	-3826.636257	-3825.281477	-1.354781	-3826.242482	-3827.597263
C19	-3826.639460	-3825.291878	-1.347582	-3826.253239	-3827.600821

Table S13. The energy components of **CBPQT**$^{4+}$ moving on **DB9**$^{3+}$ with 1 Cl^-(configuration 2)

	solution phase energy	gas phase energy	solvation energy	refined single point energy	total energy
C1	-3826.620456	-3825.343430	-1.277026	-3826.300619	-3827.577645
C2	-3826.627213	-3825.325180	-1.302033	-3826.284104	-3827.586137
C3	-3826.627039	-3825.302860	-1.324179	-3826.263236	-3827.587415
N4	-3826.613317	-3825.252110	-1.361208	-3826.215927	-3827.577135
C5	-3826.620803	-3825.238720	-1.382083	-3826.204989	-3827.587071
C6	-3826.613103	-3825.221125	-1.391977	-3826.188087	-3827.580064
C7	-3826.612357	-3825.215764	-1.396593	-3826.182125	-3827.578718
C8	-3826.605756	-3825.205148	-1.400608	-3826.172040	-3827.572649
C9	-3826.605380	-3825.195219	-1.410161	-3826.162059	-3827.572220
C10	-3826.610283	-3825.208821	-1.401462	-3826.179167	-3827.580629
N11	-3826.611839	-3825.208991	-1.402849	-3826.177801	-3827.580650
C12	-3826.610917	-3825.225561	-1.385357	-3826.188247	-3827.573604
C13	-3826.606051	-3825.227321	-1.378731	-3826.189675	-3827.568406
C14	-3826.608081	-3825.243580	-1.364502	-3826.205656	-3827.570158
C15	-3826.615778	-3825.252175	-1.363603	-3826.212390	-3827.575993
N16	-3826.635267	-3825.269363	-1.365903	-3826.229497	-3827.595400
C17	-3826.636989	-3825.276081	-1.360908	-3826.236686	-3827.597594
C18	-3826.623536	-3825.278489	-1.345048	-3826.239144	-3827.584192
C19	-3826.633095	-3825.292067	-1.341028	-3826.252559	-3827.593588

Table S14. The energy components of **CBPQT**$^{4+}$ moving on **DB9**$^{3+}$ with 2 Cl^-(configuration 1)

	solution phase energy	gas phase energy	solvation energy	refined single point energy	total energy
C1	-4286.899305	-4285.956710	-0.942595	-4287.041869	-4287.984464
C2	-4286.983289	-4286.019420	-0.963870	-4287.041869	-4288.005739
C3	-4286.980750	-4286.016829	-0.963921	-4287.040125	-4288.004047
N4	-4286.957737	-4285.968951	-0.988786	-4286.993111	-4287.981896
C5	-4286.907198	-4285.919251	-0.987947	-4286.946505	-4287.934451
C6	-4286.971718	-4285.967203	-1.004515	-4286.992011	-4287.996526
C7	-4286.973406	-4285.961970	-1.011436	-4286.987487	-4287.998922
C8	-4286.971407	-4285.959780	-1.011627	-4286.986086	-4287.997713
C9	-4286.969351	-4285.956276	-1.013075	-4286.983260	-4287.996335
C10	-4286.975694	-4285.963907	-1.011788	-4286.990521	-4288.002309
N11	-4286.968782	-4285.961263	-1.007519	-4286.989351	-4287.996871
C12	-4286.977218	-4285.979302	-0.997915	-4287.003749	-4288.001664
C13	-4286.976385	-4285.979766	-0.996619	-4287.004298	-4288.000916
C14	-4286.965867	-4285.976744	-0.989123	-4287.000805	-4287.989928
C15	-4286.960510	-4285.977385	-0.983125	-4287.001161	-4287.984287
N16	-4286.953110	-4285.977038	-0.976072	-4287.001724	-4287.977796
C17	-4286.964922	-4285.983190	-0.981731	-4287.006944	-4287.988675
C18	-4286.983461	-4285.995950	-0.987511	-4287.020131	-4288.007642
C19	-4286.981202	-4286.005775	-0.975428	-4287.028937	-4288.004365

Table S15. The energy components of **CBPQT**$^{4+}$ moving on **DB9**$^{3+}$ with 2 Cl^-(configuration 2)

	solution phase energy	gas phase energy	solvation energy	refined single point energy	total energy
C1	-4286.978759	-4286.059089	-0.919670	-4287.078379	-4287.998049
C2	-4286.968313	-4286.026128	-0.942185	-4287.047979	-4287.990165
C3	-4286.973893	-4286.017356	-0.956536	-4287.039764	-4287.996300
N4	-4286.996055	-4285.984459	-1.011596	-4287.008728	-4288.020324
C5	-4286.974522	-4285.970889	-1.003633	-4285.970894	-4286.974527
C6	-4286.972788	-4285.965110	-1.007677	-4286.992320	-4287.999998
C7	-4286.971369	-4285.961557	-1.009812	-4286.988049	-4287.997861
C8	-4286.972085	-4285.958707	-1.013378	-4286.984942	-4287.998319
C9	-4286.977769	-4285.962052	-1.015718	-4286.988930	-4288.004648
C10	-4286.974173	-4285.959666	-1.014507	-4286.986743	-4288.001250
N11	-4286.975777	-4285.959134	-1.016642	-4286.985803	-4288.002445
C12	-4286.973659	-4285.967604	-1.006056	-4286.991683	-4287.997738
C13	-4286.977459	-4285.974888	-1.002571	-4287.000449	-4288.003020
C14	-4286.973653	-4285.987052	-0.986600	-4287.013059	-4287.999659
C15	-4286.979360	-4285.994291	-0.985069	-4287.018949	-4288.004017
N16	-4286.994025	-4285.998694	-0.995331	-4287.022888	-4288.018218
C17	-4286.997505	-4286.009125	-0.988380	-4287.034257	-4288.022637
C18	-4286.986438	-4286.009549	-0.976889	-4287.032714	-4288.009604
C19	-4286.980333	-4286.011242	-0.969090	-4287.034107	-4288.003197

Table S16. The energy components of **CBPQT**$^{4+}$ moving on **DB9**$^{3+}$ with 3 Cl^-(configuration 1)

	solution phase energy	gas phase energy	solvation energy	refined single point energy	total energy
C1	-4747.299122	-4746.585479	-0.713643	-4747.665389	-4748.379032
C2	-4747.303507	-4746.611357	-0.692150	-4747.698916	-4748.391066
C3	-4747.308462	-4746.621592	-0.686871	-4747.706967	-4748.393838
N4	-4747.319485	-4746.600398	-0.719087	-4747.687947	-4748.407034
C5	-4747.331646	-4746.595618	-0.736029	-4747.684360	-4748.420389
C6	-4747.323395	-4746.606234	-0.717161	-4747.694648	-4748.411809
C7	-4747.329184	-4746.609540	-0.719643	-4747.697638	-4748.417281
C8	-4747.332382	-4746.612188	-0.720194	-4747.700471	-4748.420665
C9	-4747.331138	-4746.624271	-0.706866	-4747.712436	-4748.419302
C10	-4747.331294	-4746.625013	-0.706281	-4747.714167	-4748.420448
N11	-4747.331105	-4746.623613	-0.707492	-4747.712219	-4748.419711
C12	-4747.324684	-4746.631108	-0.693576	-4747.718225	-4748.411801
C13	-4747.397243	-4746.631009	-0.766233	-4747.717591	-4748.483824
C14	-4747.324237	-4746.634363	-0.689874	-4747.722900	-4748.412774
C15	-4747.321343	-4746.623604	-0.697739	-4747.707928	-4748.405667
N16	-4747.323576	-4746.635723	-0.687852	-4747.721061	-4748.408913
C17	-4747.339455	-4746.641968	-0.697488	-4747.727350	-4748.424838
C18	-4747.336555	-4746.642783	-0.693772	-4747.727896	-4748.421669
C19	-4747.344468	-4746.648070	-0.696399	-4747.732464	-4748.428863

Table S17. The energy components of **CBPQT**$^{4+}$ moving on **DB9**$^{3+}$ with 3 Cl^-(configuration 2)

	solution phase energy	gas phase energy	solvation energy	refined single point energy	total energy
C1	-4747.332354	-4746.694656	-0.637698	-4747.777299	-4748.414997
C2	-4747.332570	-4746.675578	-0.656992	-4747.759394	-4748.416386
C3	-4747.336101	-4746.661357	-0.674744	-4747.744694	-4748.419438
N4	-4747.342079	-4746.658042	-0.684037	-4747.742471	-4748.426508
C5	-4747.342049	-4746.652809	-0.689240	-4747.738137	-4748.427377
C6	-4747.332367	-4746.634212	-0.698156	-4747.717199	-4748.415354
C7	-4747.331877	-4746.632574	-0.699303	-4747.718283	-4748.417587
C8	-4747.335836	-4746.630539	-0.705297	-4747.719054	-4748.424351
C9	-4747.338420	-4746.635898	-0.702522	-4747.723763	-4748.426286
C10	-4747.330895	-4746.621605	-0.709290	-4747.707952	-4748.417242
N11	-4747.339561	-4746.620564	-0.718998	-4747.708176	-4748.427174
C12	-4747.328516	-4746.618773	-0.709743	-4747.705799	-4748.415542
C13	-4747.313837	-4746.615060	-0.698777	-4747.703730	-4748.402506
C14	-4747.309448	-4746.611161	-0.698287	-4747.699416	-4748.397703
C15	-4747.322918	-4746.614607	-0.708312	-4747.702723	-4748.411035
N16	-4747.349148	-4746.631216	-0.717931	-4747.717660	-4748.435591
C17	-4747.353127	-4746.635592	-0.717536	-4747.722772	-4748.440308
C18	-4747.348807	-4746.637300	-0.711508	-4747.721239	-4748.432747
C19	-4747.345710	-4746.635897	-0.709813	-4747.717481	-4748.427293

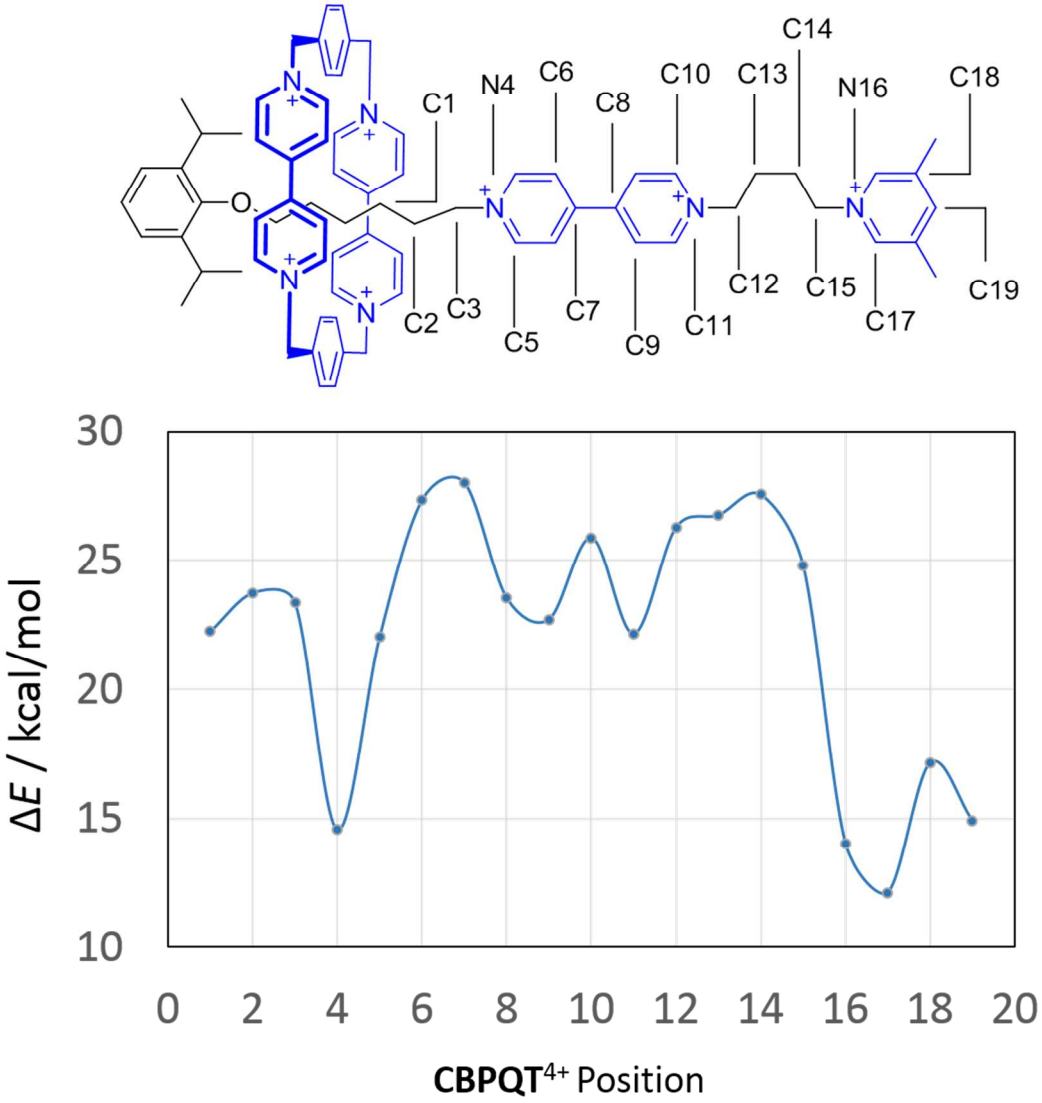

Figure S13. The potential energy surface of **CBPQT**$^{4+}$ moving on **DB9**$^{3+}$. These energies are enthalpies at 0K, except that we do not include zero point energy (the solvation correction is a free energy at 300K). The reference is at infinite separation. The energy of the rotaxane with **CBPQT**$^{4+}$ optimized with no constraint at the end of diisopropylphenol is 15.8 kcal/mol, leading to the dethreading barrier 12.4 kcal/mol. There are no experimental numbers for the dethreading of this system. However based on the comparison of theory and experiment for **DB8**$^{3+}\subset$**CBPQT**$^{4+}$ (see Figure S12) we estimate that the free energy barrier for **DB9**$^{3+}\subset$**CBPQT**$^{4+}$.is ~ 22.2 kcal mol$^{-1.}$ The discrepancy probably arises because the theory does not include ZPE or entropic affects.

7. Calculation of Energy Conversion Efficiency

Pumping one **CBPQT**$^{4+}$ from solution to a high energy state involves a three electron reduction process with Zn followed by a three electron oxidization process with Magic Blue.

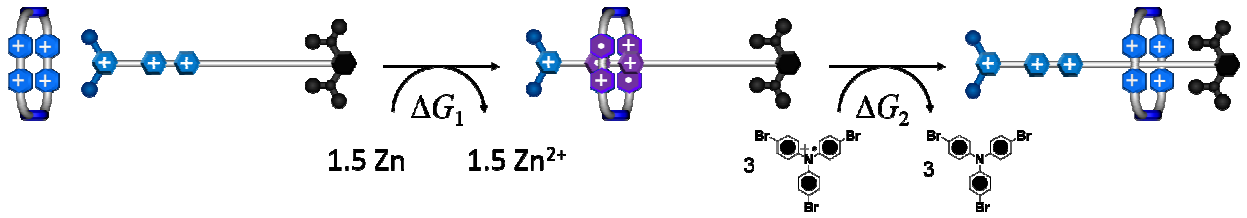

Figure S14. Energy change illustration in redox process.

The energy change in redox process can be calculated by the following equation, where n is the number of electrons transferred, $E_{Zn/Zn(II)}$ and E_{MB} are the reduction potentials for zinc and Magic Blue[8], respectively (concentration dependency is ignored for this rough calculation), and F is Faraday's constant.

$$\Delta G_1 = -nE_{Zn/Zn(II)}F = 3 \times (-0.76\ \text{V}) \times 9.65 \times 10^4\ \text{C mol}^{-1} / (4184\ \text{J kcal}^{-1}) = 52.6\ \text{kcal mol}^{-1}$$

$$\Delta G_2 = nE_{MB}F = 3 \times 1.22\ \text{V} \times 9.65 \times 10^4\ \text{C mol}^{-1} / (4184\ \text{J kcal}^{-1}) = 84.4\ \text{kcal mol}^{-1}$$

So the total energy input can be calculated as follow,

$$\Delta G_{in} = \Delta G_1 + \Delta G_2 = 137.0\ \text{kcal mol}^{-1}$$

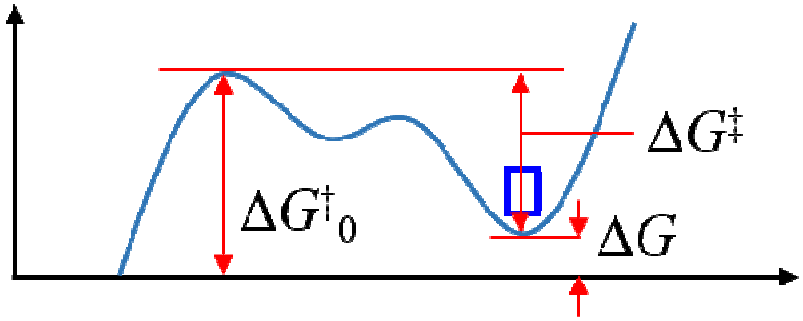

Figure S15. Energy profile for the metastable state.

Table S18. **Summary of Energy Output and Energy Conversion Efficiency.**

Species	DFT Calculated ΔH / kcal mol^{-1}	$\Delta G^{\neq}$ kcal mol^{-1}	$\Delta G^{\neq}_0$ kcal mol^{-1}	ΔG [c] kcal mol^{-1}	η [d] %
CBPQT^{4+}⊂**DB1**$^{3+}$	14.9	21.5	36 [a]	14	10
CBPQT^{4+}⊂**DB2**$^{3+}$	8.8	25.3	36 [a]	11	8
CBPQT^{4+}⊂**DB3**$^{3+}$	7.0	29.0	36 [a]	7	5
CBPQT^{4+}⊂**DB4**$^{3+}$	-	24.5	36 [a]	12	9
CBPQT^{4+}⊂**DB5**$^{3+}$	-	-	36 [a]	-	-
CBPQT^{4+}⊂**DB6**$^{3+}$	-	< 18.3	-	-	-
CBPQT^{4+}⊂**DB7**$^{3+}$	-	> 31.3	43 [b]	-	-
CBPQT^{4+}⊂**DB8**$^{3+}$	-	28.5	43 [b]	14	10

[a] Estimated based on DFT calculated ΔH for **CBPQT**$^{4+}$⊂**DB1-3**$^{3+}$ and experimental $\Delta G^{\neq}$ considering $T\Delta S$ is a small negative number. [b] Estimated based upon the experimentally observed increase of 7 kcal mol^{-1} in activation barrier upon changing a propethylene linker between the **PY**$^{+}$ and **BIPY**$^{2+}$ units to a bismethylene linker (**DB1**$^{3+}$ to **DB8**$^{3+}$) and making the assumption that their $T\Delta S$ is similar. [c] Calculated using $\Delta G = \Delta G^{\neq}_0 - \Delta G^{\neq}$. [d] Calculated using $\eta = \Delta G / \Delta G_{in}$.

8. References

1. Barnes, J. C.; Juríček, M.; Vermeulen, N. A.; Dale, E. J.; Stoddart, J. F.; *J. Org. Chem.* **2013**, *78*, 11962−11969.
2. Ikeda, T.; Higuchi, M., *Tetrahedron*, **2011**, *67*, 3046−3052.
3. Zhang, M.; Li, S.; Dong, S.; Chen, J.; Zheng, B.; Huang, F.; *Macromolecules*, **2011**, *44*, 9629−9634.
4. Trabolsi, A.; Khashab, N.; Fahrenbach, A.C.; Friedman, D.C.; Colvin, M. T.; Cotí, K. K.; Benitez, D.; Tkatchouk, E.; Olsen, J. -C.; Belowich, M. E.; Carmielli, R.; Khatib, H. A.; Goddard III, W. A.; Wasielewski, M. R.; J. F. Stoddart, *Nature Chem.* **2010**, *2*, 42−49.

5. Zhu, Z.; Fahrenbach, A. C.; Li, H.; Barnes, J. C.; Liu, Z.; Dyar, S. M.; Zhang, H.; Lei, J.; Carmieli, R.; Sarjeant, A. A.; Stern, C. L.; Wasielewski, M. R.; Stoddart, J. F., *J. Am. Chem. Soc.* **2012**, *134*, 16275—16288.
6. Tannor, D. J.; Marten, B.; Murphy, R.; Friesner, R. A.; Sitkoff, D.; Nicholls, A.; Ringnalda, M.; Goddard, W. A.; Honig, B., *J. Am. Chem. Soc.* **1994**, *116*, 11875−11882.
7. Jaguar, *Schrodinger, LLC, New York, NY* **2010**.
8. Iida, K.; Yoshida, J.; *Macromolecules*, **2006**, *39*, 6420-6424